

Intercalation of Graphene Films on Metals with Atoms and Molecules

E.V.Rut'kov and N.R.Gall

*Ioffe Physico-Technical Institute of Russian Academy of Sciences,
Russia*

1. Introduction

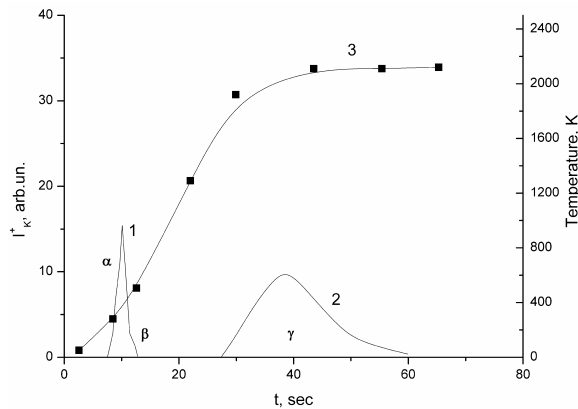
Our studies [1--3] resulted in a first observation of intercalation of graphene films on metal surfaces, which consists essentially in penetration (diffusion) of foreign atoms and molecules between the surface of a metal and the graphene film. The fact of intercalation itself implies a weak binding of graphene to the metal surface (§ 6) and finds a reasonable explanation in the graphene layer being valence saturated. Intercalation is usually observed to occur in layered solids (graphite, MoS₂) whose interlayer space may become occupied by some penetrating atoms and molecules. For instance, exposing a heated graphite crystal to cesium vapor initiates spontaneous penetration of cesium atoms between the graphite layers to form the C₈Cs intercalation compound, in which graphite layers with concentration $N_c = 3.56 \cdot 10^{15} \text{ cm}^{-2}$ alternate with cesium layers with $N_{Cs} = 5 \cdot 10^{14} \text{ cm}^{-2}$, and the distance between neighboring graphite layers increases from 3.35 Å in a graphite single crystal to 5.94 Å in C₈Cs [4, 5]. Interestingly, intercalation leaves the structure and lattice constant of the graphite layer and, hence, its individual features unchanged.

Our research group has studied in considerable detail the various aspects of intercalation of graphene films on metals with a range of atoms, more specifically, K, Cs, Na, Ba, Sr, Pt, Si, C, Ag, Al, Ir, Cu, Mo, as well as with molecules of the C₆₀ fullerenes [1--3].

2. Intercalation with atoms of alkali metals (K, Cs, Na) [1--3, 6]

2.1 Adsorption of potassium atoms on graphene-coated iridium

Potassium atoms were adsorbed at 300 K on a graphene film atop iridium to saturation, i.e., until a reverse flux of potassium atoms desorbing from the surface became equal to the incident flux. Next the surface was flash-heated. Three phases were observed in the thermal desorption spectrum (Fig. 1). The potassium atoms in the α phase desorb completely at $T < 850 \text{ K}$ are produced by desorption of potassium from graphene; indeed, the temperature of potassium desorption from the α phase matches nicely with the lifetime of potassium adatoms on graphene. The β phase having a low adsorption capacity ($\sim 10^{11} \text{ at/cm}^2$) is attributed to the potassium adatoms decorating defects in graphene films (for a more detailed account of the β phase, see [2]). The adsorption capacity of the β phase grows strongly with removal of a part of carbon atoms from the graphene film [7]. Particularly interesting is the γ phase, with potassium desorbing from this state at $T \geq 2000 \text{ K}$ (sic!) when the graphene film breaks up. This desorption phase is associated with the release of



1, 2 - α - and γ - are desorption phases, 3 - the temperature - time dependence $T(t)$.

Fig. 1. Thermal desorption spectra of K^+ ions in heating of a graphene layer on Ir(111). K was deposited at 300 K with the flux $\nu_K = 1.0 \cdot 10^{11} \text{ cm}^{-2} \cdot \text{s}^{-1}$ for 40 s.

potassium atoms buried under the graphene film. Figure 2 illustrates filling of the γ phase with potassium for $\nu_K = 6 \cdot 10^{11} \text{ cm}^{-2} \cdot \text{s}^{-1}$ reached in 10 min for different substrate temperatures in the $300 \leq T \leq 900 \text{ K}$ region, and the kinetics of this process in the 300–670 K interval is plotted in Fig. 3.

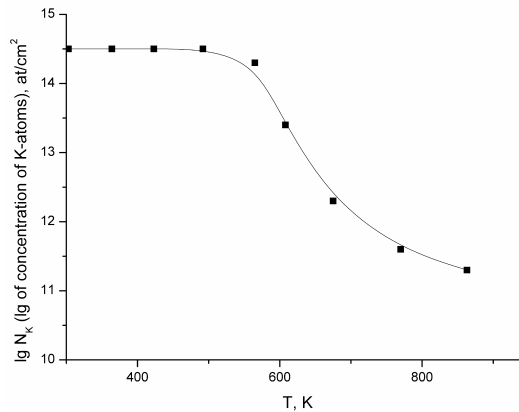


Fig. 2. K atomic concentration in logarithmic scale for K stored behind the graphene layer on Ir(111). K was deposited at various temperatures with the flux $\nu_K = 6.0 \cdot 10^{11} \text{ cm}^{-2} \cdot \text{s}^{-1}$ for 10 min at the each temperature.

In the $300 \leq T \leq 550\text{-K}$ region, the γ phase was filled in 10 min to its maximum possible level of $N_\gamma \approx (2\text{--}3) \cdot 10^{14} \text{ at/cm}^2$, which did not change during subsequent exposure to a potassium atom flux. There is more than one experimental verification of the potassium in the γ phase residing indeed under the graphene film [6]. Consider only two of them.

Verified by the work function. Potassium present with a concentration $N_K \sim (2\text{--}3) \cdot 10^{14} \text{ at/cm}^2$ on the surface of graphene was experimentally shown by CPD to reduce the surface work function by close to 2 eV. The potassium in the γ phase adsorbed to the same concentration reduces the work function by 0.3 eV only.

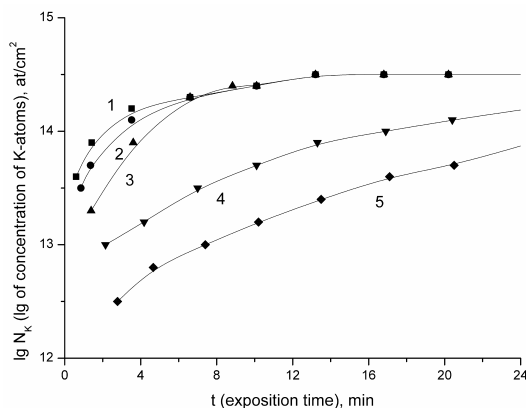


Fig. 3. K atomic concentration for K stored behind the graphene layer on Ir(111). K was deposited versus exposure time at various temperatures T (K): 1 - 300; 2 - 530; 3 - 590; 4 - 630; 5 - 670. The K flux was $v_K = 6.0 \cdot 10^{11} \text{ cm}^{-2} \cdot \text{s}^{-1}$.

Verified by AES. This is probably the most direct method of all, because it was found that filling of the γ phase with potassium to $N_\gamma \approx (2-3) \cdot 10^{14} \text{ at/cm}^2$ (following desorption of potassium from the α phase) reduces the intensity of the iridium Auger peak by a factor 1.4, although that of the carbon Auger peak does not change, thus implying that potassium is sandwiched between metal and the graphene film, i.e., resides in the intercalated state. The presence of potassium in the γ phase suggests that the graphene film is physisorbed on iridium, and that after intercalation with potassium it rose above iridium by a considerable distance, because the diameter of the potassium atom $d_0 = 4.72 \text{ \AA}$, and that of the potassium ion, $d_+ = 2.66 \text{ \AA}$ [6].

It is common knowledge that graphite can be intercalated with atoms and molecules. Obviously enough, insertion of foreign atoms between layers should increase the interplanar distance h . This is evidenced by the data [4] listed below in Table 1.

| Intercalant | Cs | K | Li | Rb | Br | HNO ₃ | HCl ₃ | FeCl ₃ |
|------------------|------|------|------|------|------|------------------|------------------|-------------------|
| $h, \text{ \AA}$ | 5,94 | 5,35 | 3,71 | 5,65 | 7,04 | 7,84 | 7,94 | 9,37 |

Table 1.

Similar results are obtained in adsorption at 300 K of Cs and Na atoms on Ir(111)-graphene.

2.2 Adsorption of potassium atoms on iridium with graphene islands

The transition from a continuous film to graphene islands brings about appearance of a number of features in thermodesorption spectra. The first of them is the sharp increase of the capacity of the β phase, which should be assigned to potassium atoms decorating the edges of graphene islands.

Second, as the area of the islands S_0 decreases, the time lag t^* in filling of the γ phase after the beginning of potassium evaporation grows rapidly. Figure 4 displays graphs illustrating γ phase filling for different S_0 . We readily see that t^* grows strongly with increasing area free of graphene islands.

Assuming all potassium atoms to roll off the graphene islands onto iridium, we find that for all S_0 filling of the γ phase starts at the same concentration of potassium on iridium, $\sim 2.5 \cdot 10^{14}$

at/cm². Significantly, in the case of a continuous graphene film on iridium, filling of the γ phase with potassium comes to completion after the concentration of atoms on the graphene surface has reached $\sim 5 \cdot 10^{13}$ at/cm².

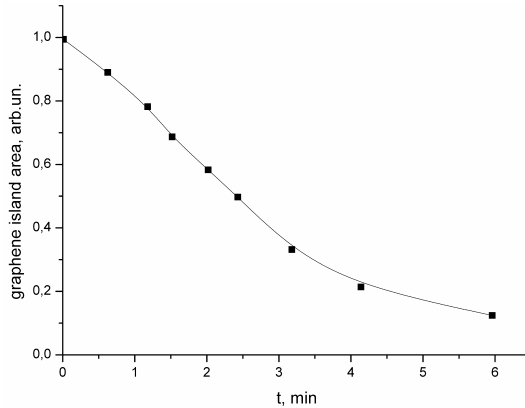


Fig. 4. Dependence of the initial time of K penetration into the γ -phase t^* versus the relative graphene island area on iridium S_0 . K was deposited at 300 K with the flux $\nu_K = 8.4 \cdot 10^{11} \text{cm}^{-2} \cdot \text{s}^{-1}$.

Figure 5 plots the dependence of the maximum filling by potassium of the γ phase on the relative area of graphite islands. We see N_γ to scale directly proportional to S_0 .

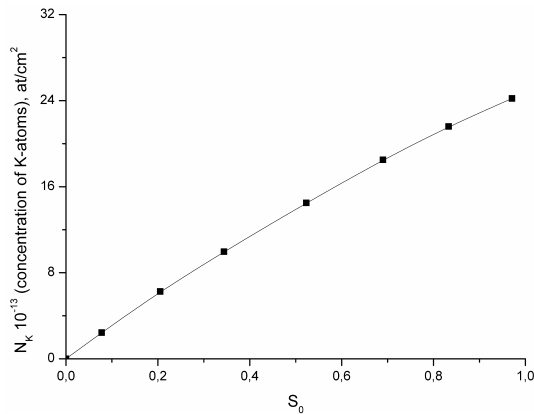


Fig. 5. Maximal K concentration under graphene (in the γ -phase) N_K versus the relative island area on Ir(111). K was deposited at 300 K with the flux $\nu_K = 2.0 \cdot 10^{12} \text{cm}^{-2} \cdot \text{s}^{-1}$. N_K was determined by TDS method.

Consider now how could one explain these results. Obviously enough, the first centers to be filled by adsorbing potassium atoms should be those with strong binding; here they would be edges of the graphite islands (the β phase). The next to be filled are less energetically favorable centers; potassium adsorbs on iridium. For $\theta > 0.1$, a substantial part should be played by Coulomb repulsion among positively charged potassium adatoms, and it is apparently this repulsion that prevents complete filling of the potassium monolayer on

iridium, so that for $N_K \geq 2.5 \cdot 10^{14}$ at/cm² potassium atoms acted upon by Coulomb forces will start occupying the free surface of graphene islands. This is followed by effective filling of the γ phase. Just as in the case of a continuous graphene film, potassium from the γ phase for graphene islands desorbs from the surface at high temperatures ($T \geq 1900$ K). That potassium persists for a long time at high temperatures in the γ phase suggests that valence-non-saturated carbon atoms at the edges of graphene islands are chemically bound to atoms in the surface layer of iridium. It is the closed island edges that prevent potassium from escaping from under the islands ("bottom-up saucer" island, Fig. 6).

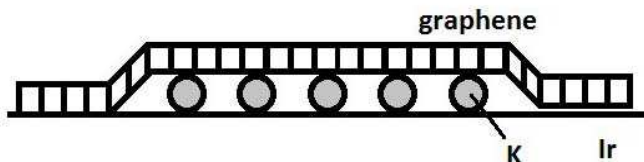


Fig. 6. Schematic graphene island on a metal with atomic K in the γ -phase.

5.3 Adsorption of cesium atoms on graphene atop rhenium [7--11]

One more example of a substrate metal, rhenium, may be in order here to demonstrate that graphene islands are physisorbed in this case too. A rhenium ribbon was carbonized in benzene vapor at $T_c = 1700$ K up to formation of a graphene film, after which the temperature was lowered to 300 K by turning off the heating current. Experiments showed that in this way one can preserve a graphene layer on iridium at temperatures of 300--1100 K, because volume diffusion becomes frozen at these temperatures. Thereafter, cesium atoms were adsorbed at 300 K on the graphene layer atop iridium in a constant flux $v_{Cs} = 2 \cdot 10^{12}$ cm⁻²s⁻¹ to saturation, i.e., until the reverse flux became equal to the incident one. After this, the temperature was flashed (Fig. 7). We readily see that cesium desorption occurs in two phases, with the first of them (α phase) observed at $T \sim 900$ K, and the second (γ phase), at high temperatures, $T \geq 2100$ K (sic!). The temperature of cesium desorption from the α phase matches with the lifetime of cesium on a graphene film (§ 7) and can be identified with cesium escaping from the surface of the graphene film. The high temperatures of cesium desorption from the γ phase are associated with cesium becoming freed from under the graphene film when it breaks up. The maximum adsorption capacity of cesium in the γ phase, $N_\gamma \approx 8 \cdot 10^{13}$ at/cm². Significantly, in these experiments the adsorption capacity of the β phase of cesium (similar to the potassium β phase for the iridium-graphene system), which is related with graphene defects, was at a level of $N_\beta \sim 10^{11}$ at/cm², and is not reflected in Fig. 7. Just as for the Ir-C system, we are going to present here two arguments in support of cesium in the γ phase being buried under the graphene film.

1. The work function of the surface of a graphene film decreases after maximum filling by cesium of the γ phase by ~ 0.25 eV, although the same amount of cesium present in the α phase causes a decrease of the work function by ~ 1.25 eV.
2. After desorption of the cesium α phase, the Auger peak intensity of carbon recovers to the level corresponding to a clean graphene film, whereas the rhenium peak intensity is found to be lower by a factor ~ 1.3 than that before the beginning of cesium adsorption. This implies that cesium in the γ phase is sandwiched between the graphene film and the metal.

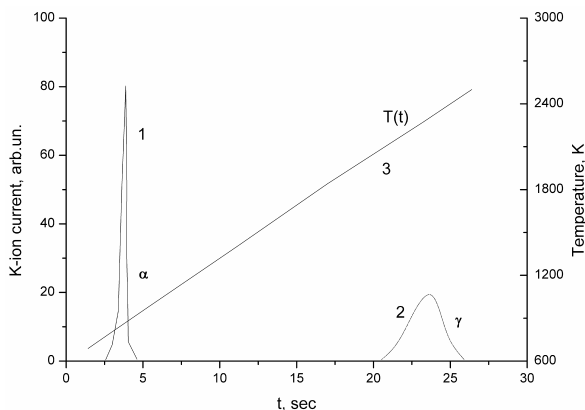


Fig. 7. Thermal desorption spectra for Cs⁺ ion after Cs deposition on a graphene layer on Re. Cs was deposited at 300 K with the flux $\nu_K = 8.5 \cdot 10^{11} \text{ cm}^{-2} \cdot \text{s}^{-1}$ for 15 min. 1, 2 - α - and γ -desorption phases, 3 the temperature - time dependence $T(t)$.

Figure 8 illustrates filling of the γ phase by evaporation of cesium atoms for $\nu_{\text{Cs}} = 3.3 \cdot 10^{12} \text{ cm}^{-2} \cdot \text{s}^{-1}$ during 10 min, measured for different substrate temperatures within the interval $300 \leq T \leq 900 \text{ K}$. Examining Fig. 8, we see that intensive filling of the γ phase by cesium starts at $T \leq 800 \text{ K}$. Just as in the case of potassium atoms, the maximum adsorption capacity of the cesium γ phase does not depend on the sample exposure time to the flux of cesium atoms.

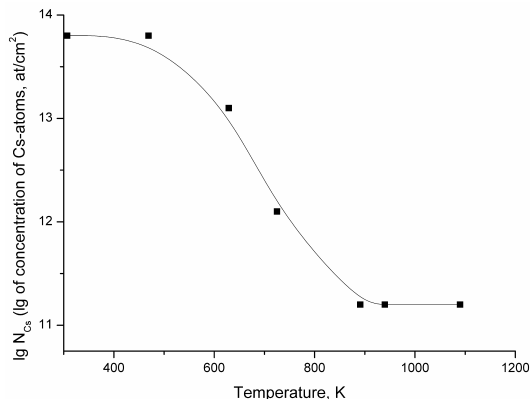


Fig. 8. Cs atomic concentration in logarithmic scale for Cs stored behind the graphene layer on Ir(111) versus temperature. Cs was deposited at various temperatures with the flux $\nu_{\text{Cs}} = 3.3 \cdot 10^{12} \text{ cm}^{-2} \cdot \text{s}^{-1}$ for 10 min at the each temperature.

Thus, the assumption of a graphene film on a metal being physisorbed is valid not only for iridium but for rhenium as well. Similar experiments on adsorption of K, Na, and Cs atoms performed on graphene grown atop other metals as well---rhodium, molybdenum, platinum, and nickel, provide convincing support for the general physisorptive character of graphene bonding with a metal surface.

2.4 Intercalation of graphene on a metal with alkali atoms [2, 3, 12, 13]

Application of TDS (in studies of adsorption of Cs atoms on graphene atop rhenium) involving detection of the ions released in surface ionization increased strongly the sensitivity of the method in the initial stages of adsorption, when the surface work function does not yet change and each desorbing Cs atom escapes in the form of the Cs⁺ ion.

The following features observed at $T = 300$ K appear noteworthy.

1. At cesium concentrations on graphene atop rhenium below $N_{Cs} \approx 1 \cdot 10^{12}$ at/cm², cesium atoms reside only in the α phase, i.e., on the surface of the graphene film.
2. For $N_{Cs} > 1 \cdot 10^{12}$ at/cm², surface migration of cesium atoms sets in (rather of cesium ions, because cesium on the surface is positively charged), which is apparently initiated by Coulomb repulsion. In the process, cesium transfers to the back side of the ribbon to the α state, which is corroborated by the observation that the thermodesorption spectrum contains only the α phase with the cesium concentration $N_{Cs} = \frac{1}{2}v_{Cs}t_{exp}$.
3. After the cesium concentration on both sides of the rhenium ribbon has reached the level $N_{Cs} \geq 1 \cdot 10^{13}$ at/cm², cesium atoms start to diffuse actively into the space under graphene, signaling filling of the γ phase. The total concentration of cesium on the surface becomes $N_{Cs}(tot) = \frac{1}{2}v_{Cs}t_{exp}$, because half of the material (cesium) escapes to the back side of the ribbon (this is why the α and β phases of cesium on the front side of the ribbon are easy to fill by evaporating it on the back side of the sample). It is apparently only at noticeable cesium concentrations ($\geq 1 \cdot 10^{13}$ at/cm²) that the forces of electrostatic repulsion among cesium adatoms with a charge close to 1 become strong enough to overcome an activation barrier and start to diffuse under the graphene film. The nature of this activation barrier remains unclear, but it could be related, for instance, with the Coulomb repulsion of the cesium adatom from a positively charged defect in a graphene film, and it is possibly this defect that mediates efficiently the escape of charged adatoms migrating over the surface.

The process of filling of the γ phase by the other alkali atoms, sodium and potassium, exhibits basically the same features as that of the filling by cesium, which should be assigned to these alkali atoms having a noticeable positive charge on the graphene surface.

Cs, Na, and K atoms fill actively the γ phase in the 300--700-K temperature interval, where evaporation of atoms can result in building up on the surface of a certain "critical" concentration of adatoms which would initiate filling up of the γ phase. For $T > 700$ K, the lifetimes of alkali metals on graphene become too short (§7), which reduces the equilibrium surface concentration, with the result that the migration transfer under the graphite layer drops sharply (Figs. 2 and 8).

2.5 Why do Cs atoms find it easy to diffuse under the graphene film but hard to escape from under it?

There are presently no grounds to doubt that adatoms of alkali metals are "pushed" under the graphene film by their electrostatic repulsion. It was observed that for the intercalation of single-crystal graphite by alkali metals to begin, they should first build up to a certain concentration on the crystal faces [14]. This reminds one of the problem where one should force into a rubber tube balls of a slightly larger diameter; it can be solved by applying a certain force F (Fig. 9A). As the pushing "finger" acts in our case repulsion among positively charged adatoms (Fig. 9B). The above is supported by experiments aimed at studying Cs migration under the graphene islands; indeed, single Cs adatoms were found to practically not migrate under graphene at all [15].

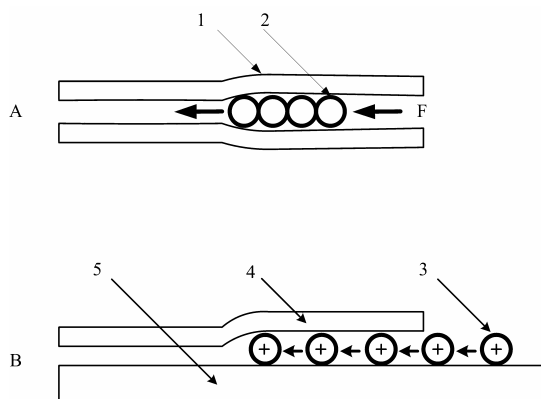


Fig. 9. **A.** Schematic structure of solid balls movement inside a ribbon tube under the action of an external force: 1 – ribbon tube, 2 – solid ball. **B.** Schematic structure for electropositive atomic metal penetration between the graphene layer and metal substrate: 3 – adsorbed Cs, 4 – graphene layer, 5 – metal substrate.

Now about the question of why it is easy ($T = 300$ K) for atoms of alkali metals to transfer under a graphene film but difficult (at $T \geq 2000$ K!) to escape from under it, i.e., why the entry--escape ways are so strongly asymmetric.

Studies of the intercalation of graphene on Rh(111) with Cs atoms revealed that after desorption of the Cs α phase from the graphene surface, the cesium intercalant emerges partially from under the graphene film and desorbs likewise at low temperatures, 900--1000 K. The emergence of cesium from under graphene is signaled by the formation of diffusion "tails" in thermodesorption spectra (Fig. 10).

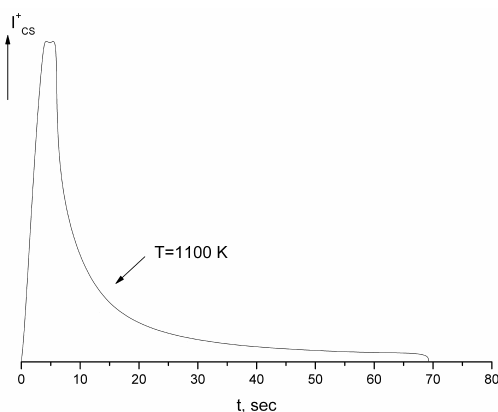


Fig. 10. Thermal desorption spectroscopy for Cs⁺ ions from the graphene layer on Rh(111) in the temperature increase from 300 to 1100 K. Cs was deposited at 300 K up to the concentration $N_{Cs} = \nu_{Cs} \cdot t = 4.4 \cdot 10^{14} \text{ cm}^{-2}$.

Significantly, the larger was the amount of Cs adsorbed into the α phase, the deeper penetrated Cs atoms and in larger numbers under the graphene layer, and the longer was the diffusion "tail" in the TDS spectra.

Thus, as T increases, Cs emergence from under the layer is initially not blocked in any way, which makes it difficult to separate the α phase of the Cs emergence from the onset of the Cs escape from the γ phase. We are turning now to the second question of what forced adatoms to stay in intercalated state, so that they escape from under the graphene film only when it breaks up, and this may require quite high temperatures, often above 2000 K (sic!).

The answer to this question may be contained in Fig. 11. As T increases, Cs escapes from the α phase, i.e., from the graphene surface (1 in Fig. 11A), the next to desorb is Cs from the defects in the layer (2 in Fig. 11B), and it is through them that adatoms penetrate under the layer in the first place. The turn to emerge comes after that to Cs adatoms bound close to graphene island edges (3 in Fig. 11C). The Cs adatoms left far from the layer edge do not have time enough to migrate to the edge closing to the metal (4 in Fig. 11D). These adatoms remained trapped under the “bottom-up saucer” islands (Fig. 6).

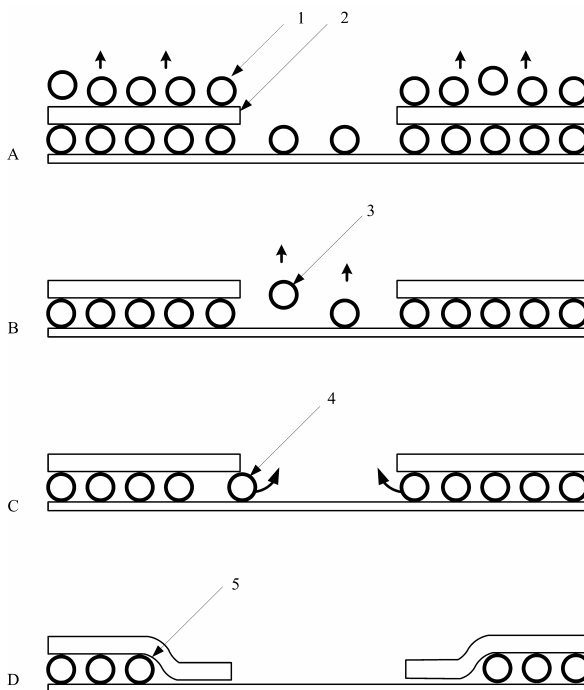


Fig. 11. Schematic model (A - D) showing the process of Cs liberation from the γ -phase and the island edge closure to the metal substrate after the temperature increase for the intercalation system Me-Cs-graphene. 1 - atomic Cs above the graphene layer, α - phase; 2 - graphene; 3 - atomic Cs desorbing from the layer defect; 4 - intercalated Cs near the island edge; 5 - 'locked' atomic Cs under the layer; graphene traps.

2.6 Excitation of edges of graphene islands

Under certain temperatures, the graphene island edges bound to metal should open periodically stimulated by thermal excitation. Rupture of the Me-C chemical bond may open the way for a part of the intercalant cesium to escape from under the graphene film and desorb. This accounts for a certain, albeit low-density, flux v_{Cs} of Cs atoms leaving at $T >$

1000 K. For instance, for the Ir(111)-graphene system with a cesium concentration under graphene $N_V \sim 2 \cdot 10^{14}$ at/cm² and $T = 1100$ K, $v_{Cs} \sim 10^9$ – 10^{10} cm⁻²s⁻¹. The Cs flux decreases with time, primarily because of the edge region becoming depleted in cesium, which makes it ever more difficult for the remaining adatoms to reach the island edge. Experiments demonstrate that removing Cs from under a graphene film without destroying it takes up several hours at $T \sim 1100$ K on Ir(111), although the lifetime of Cs, both on graphene and on iridium, at this temperature is only ~ 0.01 s (§ 7).

Figure 12 plots the variation of the flux of Cs atoms emerging from under graphene on Rh(111) with the substrate temperature varied from $T_1 = 1300$ K to $T_2 = 1350$ K, for the Cs concentration under the graphene islands $N_{Cs}(V) = 5 \cdot 10^{13}$ at/cm².

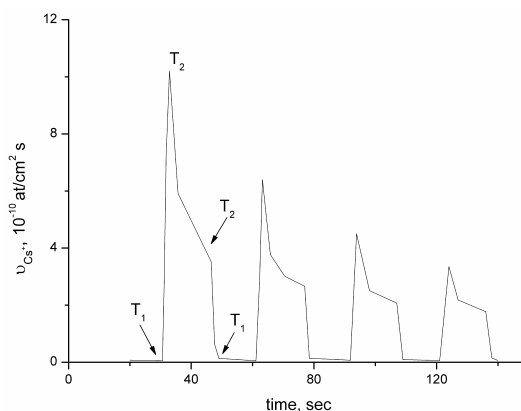


Fig. 12. The flux of Cs⁺ ions out of graphene islands in their thermal excitation. The temperature was $T_1 = 1300$ K and $T_2 = 1350$ K, relative island area was $s_0 \sim 15\%$. The islands were grown on Rh(111), and Cs was intercalated to saturation at 300 K.

We immediately see a sharp rise of the cesium flux with increasing temperature associated with the increase of thermal excitation of graphene. As the temperature returns to its initial level T_1 , the cesium flux density falls off rapidly too. Experiments with cyclic variation of temperature $T_1 \rightarrow T_2 \rightarrow T_1$ can be performed many times, and the results will be the same, except for the gradual decrease of the burst in the flux density of Cs atoms escaping from under the graphene (Fig. 12).

Knat'ko *et al.* [1989] showed that illumination with light or electron bombardment of a graphene film on Cs-intercalated iridium heated to ~ 900 K initiates emergence of these adatoms from under the graphene islands, which was visualized by monitoring the Cs⁺ current. This effect was observed at photon energies varied from 2.3 to 1.5 eV, with the low-energy threshold remaining not quantified. It was assumed that the adatoms escape from under the graphene islands through some "valves" forming in the rupture of bonding of island-edge C atoms with iridium initiated by irradiation by light or electrons. The transport of particles taking place in the absence of external stimulating factors was explained as due to diffusion via defects present in the graphene film. The kinetics of these processes stimulated by light and electrons was studied, and a model reproducing them proposed [15]. It was shown that the burst of the Cs⁺ ion current can be attributed to the emergence of adatoms buried under graphene close to the island edges. Filling of the near-edge region after its having being depleted by irradiation is a very slow process, which sets in probably

following formation of a compact Cs cluster diffusing as a whole to the edge of an island from its central region. Thus Knat'ko *et al.* [1989] established an unusual pattern of migration of intercalated Cs atoms, in that they move in compact clusters rather than singly, with the rate of migration growing with increasing concentration of the intercalated atoms.

Besides the edges of graphene islands, thermal excitation may set in in any part of an island, accompanied by the appearance of a graphene hillock and increase of the graphene-metal distance at this point [16].

Even at $T = 300$ K, one may expect excitation of any part of graphene islands bound with the metal by weak van der Waals forces; indeed, such bubbles form and disappear all the time over the film. It appears reasonable to assume that from time to time, each carbon atom in the graphene network, is capable, while participating in thermal random motion, of building up on the bond with the surface an energy high enough to be able, in moving away from the surface, to drag along its nearest neighbors and form a graphene "bubble".

A graphene film could be said to remind one, as a suitable figure of speech, the surface of a rough sea, with crests and hollows coming to life and disappearing continuously, with the sea roughness becoming the stronger, the stronger is the gale (the temperature in the case of graphene).

Tontogode (1985) [16] resorted to the relation of Frenkel $\tau = \tau_0 \exp(E/kT)$ to estimate the kinetic energy E building up on a particle bond in random thermal motion in a given observation time τ at a temperature T , which is expended in formation of a "bubble". In this sense, the motion of a carbon atom over the network on the surface resembles largely the process of desorption, the only difference being that the graphene network itself, not unlike a spring, restores the carbon atom to its original position.

Estimates show that for a binding energy of a carbon atom with the metal in a graphene film of ~ 0.2 eV, a graphene "bubble" should accumulate four atoms in a time $\tau = 1$ s (for $\tau_0 = 10^{-13}$ s) at $T = 300$ K, while at $T = 1500$ K the "bubble" will be quite large and contain ~ 20 atoms. Formation of graphene "bubbles" facilitates migration of intercalated atoms.

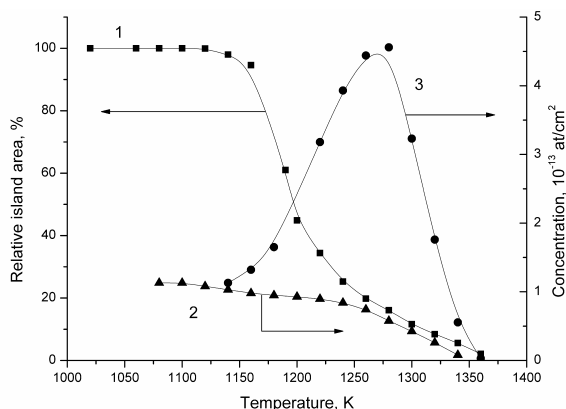
2.7 Compression of a layer of Cs atoms under graphene islands

The first successful monitoring of the area of graphene islands with carbon atoms trapped underneath was made in the course of their destruction. The experiment started with intercalation of a graphene film on rhodium at 300 K with cesium atoms. Next the cesium was removed from the surface at ~ 900 K, after which the temperature was raised to $T_1 > 1250$ K, and the relative island area S_{01} was determined. Next the surface was flash heated, and the amount of cesium N_1 under the islands of area S_{01} deduced. The experiment was repeated from the very beginning, but now the temperature was raised to $T_2 > T_1$, the magnitude of $S_{02} < S_{01}$ found, and N_2 derived. The results obtained are summarized graphically in Fig. 13A, in which each data point is essentially a separate experiment.

We readily see that a decrease of the relative island area from 100% (continuous layer) to $\sim 20\%$ (curve 1 in Fig. 13A) does not actually entail a noticeable decrease of the total number of cesium atoms on the surface (curve 2 in Fig. 12A). This implies that while the islands may shrink markedly in area, they do not "let go" the cesium atoms buried under them (Fig. 13B). It is as obvious also that although the number of cesium atoms under the islands remains unchanged, their concentration grows through the decrease of islands in area (curve 3 in Fig. 13A for $T = 1150$ – 1270 K).

We note also that for $T > 1300$ K graphene islands become so small that they can possibly no longer keep trapped the cesium atoms confined under them, with the result that the average concentration of intercalated cesium will start to decrease. Apart from this, the concentration

A.



B.

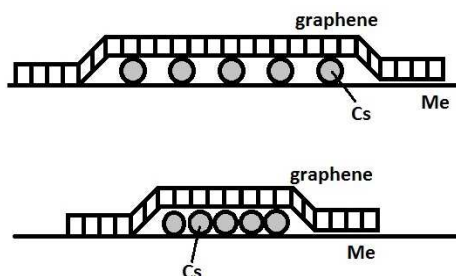


Fig. 13. Compression of graphene islands with intercalated Cs. **A.** Temperature dependences of: 1 - relative graphene island area; 2 - Cs concentration relative the total surface area; 3 - calculated Cs concentration relative to the actual area occupied by graphene. **B.** Schematic structure of the process:

of the graphene islands themselves will decrease as they break up with increasing temperature. Recalling the well known expression for particle lifetime on the surface, $\tau = \tau_0 \exp(E/kT)$ (τ_0 is the prefactor, E , the desorption energy, is in our case $E \sim 2$ eV [17]), we come readily to the estimate that graphene traps increased the lifetime of cesium adatoms on rhodium surface $\sim 10^6$ times.

Thus, we have revealed a new effect inherent in intercalation of an alkali metal under graphene films and consisting in a substantial increase of its concentration in the intercalated state under heating of the adlayer. While annealing reduces the graphene island area, their edge atoms bound with the metal by chemisorption forces do not let cesium emerge from under the graphene; this gives rise to compression of the cesium layer, and it is under the islands that its surface concentration exhibits a noticeable increase.

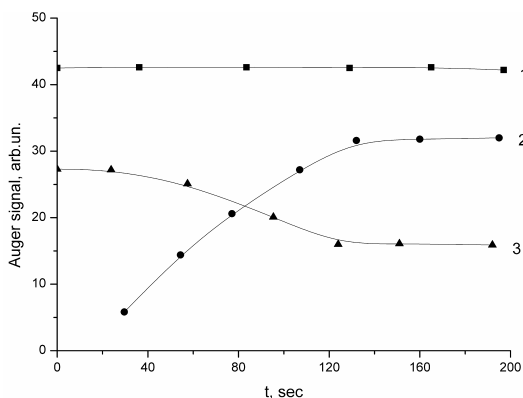
3. Intercalation with barium [18, 19]

It was found that Ba intercalates under graphene on iridium and rhenium, but the pattern of the processes involved depends essentially on the temperature of the substrate metal. We are going therefore to consider these processes separately for $T < 1000$ K and $T > 1000$ K.

3.1 Adsorption of Ba on Ir-C for $T < 1000$ K

In the case of Ba adsorbed on iridium at 300 K intercalation does not seem to occur, which can be deduced from a characteristic change in shape of the carbon $C_{k_{VV}}$ Auger peak (to be discussed in detail below), but because of strong Ba-Ba bonding on the graphene surface Ba undergoes condensation, which complicates monitoring the intercalation process. Adsorption of Ba on iridium at 300 K does not probably result in intercalation, which is suggested by a characteristic change in the shape of the $C_{k_{VV}}$ Auger peak of carbon (to be discussed in detail below), but strong Ba-Ba binding gives rise to condensation of Ba on graphene surface, which makes difficult monitoring the intercalation processes. These difficulties are sidestepped by invoking adsorption of Ba on heated Ir-C. Consider Fig. 14A, displaying the dependence of the Ba, Ir, and C Auger peak intensities observed in Ba adsorption on Ir-C at 880 K. In the course of adsorption, the Auger peak of Ba grows in amplitude and that of iridium falls off, while the carbon Auger peak does not change. This implies that barium accumulates only under the graphene as intercalant (Fig. 14B). For $t \geq 150$ s, the concentration of intercalated Ba becomes as high as $5 \cdot 10^{14} \text{ cm}^{-2}$ (which is close to its monolayer concentration on the surface of transition metals) and changes no more. The efficiency of intercalation is ~ 0.3 , in other words, 30% of the Ba flux striking the Ir-C surface becomes intercalated, with the remaining 70% desorbing. If we heat now this system, approximately 50% of the intercalated barium desorb at $T \leq 1300$ K, while the barium left under the graphene with the concentration of $2 \cdot 10^{14} \text{ cm}^{-2}$ leaves the surface only at $T > 2000$ K, when the islands break up. This experiment provides one more argument for the absence of any "blocking" of Ba escape from under graphene in the initial stage, as this was observed in the case of cesium.

A.



B.

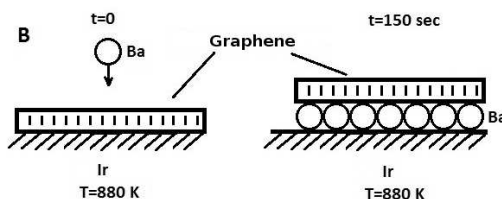


Fig. 14. Ba intercalation under a graphene layer on Ir(111). A. Auger signals of carbon (1), barium (2), and iridium (3) versus total amount of deposited Ba onto Ir-C at 880 K. The deposition flux is $\nu_{Ba} = 3.2 \cdot 10^{12} \text{ cm}^{-2} \cdot \text{s}^{-1}$. B. Schematic structure of the process:

3.2 Adsorption of barium on Ir-C at $1000 < T < 1500$ K

Ba atoms with activation energy for desorption $E = 1.9$ eV desorb intensively from graphene on iridium at 880 K. Therefore observation of existence of barium islands on Ir-C at substantially higher temperatures, $1000 < T < 1500$ K, came as a total surprise [19]. One studied the specific features of growth and dissolution of two-dimensional barium islands on Ir-C [17, 21]. Barium in these islands was bound strongly with the substrate with an energy of 3.4 eV and was present in a concentration of $2 \cdot 10^{14}$ cm⁻², which means that the Ba islands were not close packed. In this temperature region, Ba did not intercalate with graphene. One had to account for the high binding energy of barium with the substrate in an island, 3.4 eV, which exceeds substantially the energy required for Ba sublimation, ~ 1.8 eV, and that for desorption of a Ba atom from Ir-C, which is 1.9 eV. We assumed that Ba adatoms are adsorbed at the centers of benzene rings in the graphene film, so that when the latter performs random thermal vibrations, they come closer to the surface atoms of iridium and compress slightly the graphene film to form an electron bond with iridium with a binding energy increased from 1.9 to 3.4 eV (Fig. 15). It appears actually a reasonable assumption, because the energy of desorption of a Ba atom from the iridium surface is high, 5.7 eV. If such a Ba monolayer is heated to $T \sim 1600$ K, about half of the barium will desorb, while the other half will migrate under the film to become an intercalant. If now we adsorb Ba again at $1000 < T < 1500$ K on graphene confining intercalated barium in a concentration of $5 \cdot 10^{13}$ cm⁻², strongly bound Ba islands do form, but only on a part of the surface [18]. It appears probable that the intercalated Ba is distributed nonuniformly in these experiments, so that regions with its maximum concentration of $5 \cdot 10^{14}$ cm⁻² border areas with no intercalated Ba present, but it is in these regions that strongly bound Ba islands form on graphene (Fig. 16). At concentrations of intercalated Ba in excess of $2 \cdot 10^{14}$ cm⁻², strongly bound islands do not form at all. Neither do they form on the surface of a graphene film on iridium at film thicknesses above two monolayers. Similar results were obtained by us in studies of strontium adsorption on Ir-C [18--21].

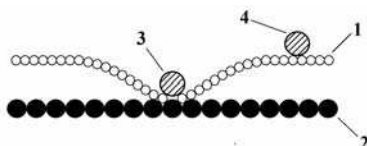


Fig. 15. Schematic structure of the graphene layer (1) on iridium (2) with strongly (3) and weakly (4) bonded atomic Ba.

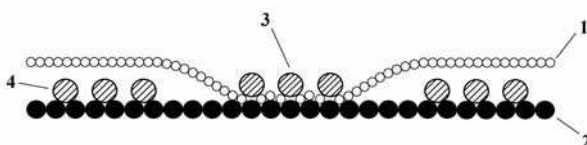


Fig. 16. Schematic structure of the graphene layer (1) on iridium (2) with 2D Ba island (3) and intercalated Ba (4).

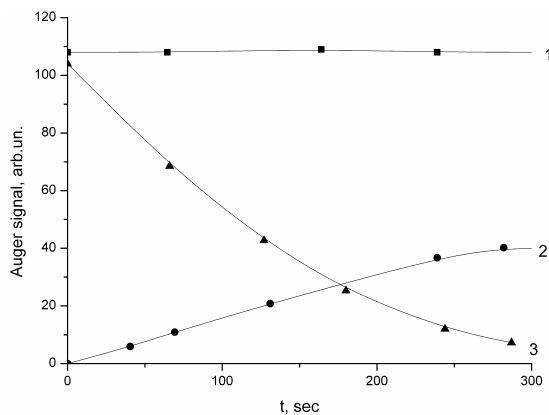
4. Intercalation with platinum [22]

It was found that a graphene film on a metal is intercalated efficiently with atoms having low ionization potentials (Cs, K, Ba,...), which are positively charged on graphene and are strongly

bound with it by mirror image forces. An intriguing question arises immediately of whether atoms with high ionization potentials, which are not charged on a graphene film and bound with it only weakly by van der Waals forces of polarization origin, would intercalate a graphene film on a metal. In an attempt at finding an answer to this question, we studied adsorption and intercalation of Ir-C with atoms of Pt, Si, and C.

Platinum was evaporated by sublimation from heated Pt ribbons. Pt adsorbed on Ir-C at 300 K grew to form a thick film on the graphene film. It was found that Pt atoms adsorbing on a graphene film atop iridium heated to 1000 K intercalate with Ir-C with an efficiency $\kappa = 1$. This intriguing result implies that *each* Pt atom incident at 1000 K on a graphene film penetrates under it to become an intercalant species. Figure 17A shows how the Auger peaks of carbon, platinum and iridium vary as a result of adsorption of Pt on Ir-C at a higher $T = 1200$ K, when the intercalation efficiency is slightly lower ($\kappa < 1$), and part of Pt atoms desorb from the graphene film. Interestingly, in contrast to Cs, K, and Ba atoms which form in intercalated state a monatomic film, Pt grows under the graphene in a thick, *multilayer* film, which, on the one hand, is strongly chemically bound with iridium, while on the other is coupled weakly, probably by van der Waals forces, to the graphene film (Fig. 17B). This is probably what accounts for our observation [2, 3] of the effect of *bi-intercalation*, in which consecutive adsorption first of Pt atoms, and subsequently, by atoms of Cs, brings about growth under the graphene film of a thick Pt film, with a Cs monolayer forming on top of it (Fig. 18).

A.



B.

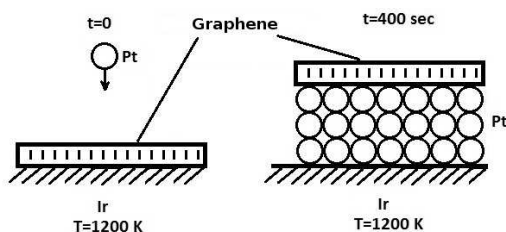


Fig. 17. Pt intercalation under a graphene layer on Ir(111). **A.** Auger signals of carbon (1), Pt (2), and iridium (3) versus Pt deposition time onto Ir-C at 1200 K. The deposition flux is $v_{Pt}=1 \cdot 10^{13} \text{ cm}^{-2} \cdot \text{s}^{-1}$. **B.** Schematic structure of the process:

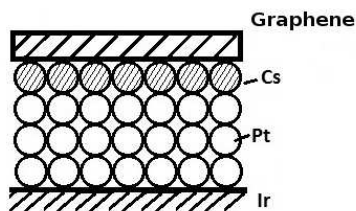


Fig. 18. Schematic structure of the layer in bi-intercalation: first Pt is deposited onto the graphene layer on Ir(111) at 1000 K; then Cs was deposited at 300 K and the system was annealed at 800 K to remove α -phase Cs.

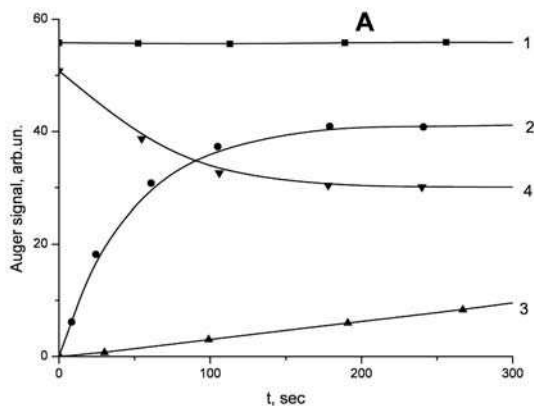
The condition $\kappa = 1$ means that a Pt atom physisorbed on graphene can migrate in its lifetime against desorption from the center of the island to its edge, which is possible if migration over graphene is very efficient. For the process to be efficient enough, the graphene film should be smooth, and the potential relief for migration, fine; also, the graphene islands should not be very large. Because Pt adatoms on graphene residing atop iridium are electrically neutral, decoration of the graphene island edges by them leaves it neutral, as a result of which intercalation with Pt occurs without the concentration threshold characteristic of the intercalation with Cs, K, and Ba; this means that already the very first Pt atoms adsorbing on graphene with iridium heated to 1000 K penetrate under the film. Interesting data were obtained on the efficiency of intercalating Ir-C with Pt atoms at lower temperatures, $300 < T < 1000$ K, as well. For instance, if platinum is evaporated on a graphene film on iridium at 300 K, then at room temperature no intercalation is observed; instead, Pt is adsorbed to form a monolayer (with $N_{Pt} \sim 1 \cdot 10^{15} \text{ cm}^{-2}$, which reduces the Auger peak of carbon (with $E = 272 \text{ eV}$) by a factor 1.5, and that of iridium ($E = 54 \text{ eV}$), ~ 3 times. After this, the temperature was raised in steps of 100° , with exposure of the sample for 30 s at each temperature. As the temperature increased, the Auger peak of iridium was found not to change, while that of carbon grew by a factor 1.5. This means that as the temperature was raised, all of the adsorbed Pt monolayer became intercalated, apparently already at $T < 1000$ K, when Pt does not yet start to desorb.

5. Intercalation with silicon [2, 3, 22]

Silicon was deposited by sublimation from heated ribbons. Si adsorbed on Ir-C at 300 K grows to form a thick film which reduces the Auger peaks of carbon and iridium until they melt into the background. As T increases, the pattern of carbon film growth changes substantially, Figure 19A plots the variation of the intensities of Auger peaks of carbon, silicon, an iridium in the course of Si adsorption on Ir-C at 1000 K. The growth of the silicon Auger peak suggests that silicon builds up in the near-surface region, and the constancy of the carbon peak, that silicon accumulates under the graphene film. After 150 s of deposition, the Auger peaks of silicon and iridium stop to change, hence, stops to change also the composition of the near-surface region $\geq (10\text{--}15) \text{ \AA}$ thick, which is accessible for AES. Studies of silicon adsorption on clean iridium [23] revealed that up to the concentration $N_{Si} \sim 3 \cdot 10^{14} \text{ cm}^{-2}$ all of the silicon incident on the surface accumulates in the form of a surface chemical compound, surface silicide. Silicon atoms arriving onto the surface after this state has been filled diffuse into the bulk of iridium to form in its near-surface region volume silicide (Fig. 19B). It was found that the curves plotting the variation of the silicon Auger peak intensities

vs. deposition time of the same silicon flux on iridium and iridium coated by a graphene film at 1000 K practically coincide (if one accounts for the attenuation of the silicon Auger peak intensity by the graphene film). This means that silicon intercalates into Ir-C at 1000 K with an efficiency $\kappa \sim 1$. When Si adsorbs on Ir-C at higher temperatures $T \geq 1300$ K, a sizable part of it becomes bound in the intercalated state, with the remainder desorbing.

A.



B.

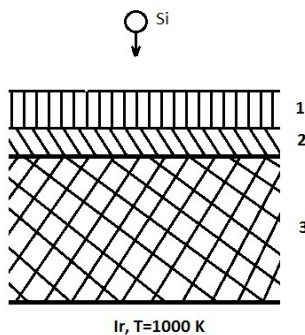


Fig. 19. Si intercalation under a graphene layer on Ir(111). **A.** Auger signals of carbon (1), Si (2), and iridium (4) versus Si deposition time onto Ir-C at 1000 K. (2) - Si Auger signal in its deposition onto Ir-C at 1500 K. The deposition flux is $v_{\text{Si}} = 1 \cdot 10^{13} \text{ cm}^{-2} \cdot \text{s}^{-1}$. **B.** Schematic structure of the process: 1 - graphene layer; 2 - surface silicide; 3 - bulk silicide

6. Intercalation with carbon [2, 3]

The experiments which demonstrated that atoms of Pt and Si intercalate with an efficiency $\kappa = 1$ under a graphene film adsorbed on iridium heated to $T = 1000$ K stimulated interest in looking for other atoms which could be intercalated with intrinsic carbon atoms. In these experiments, carbon atoms (emitted by a source developed by us and not producing C clusters [24]) were deposited at $300 < T < 1800$ K on a graphene film atop iridium, with the film thickness probed by AES. At all these temperatures, a thick carbon film was observed to

grow, but its nature (graphitic or non-graphitic) and the growth mechanism involved were found to depend strongly on T .

Adsorption of C atoms on a graphene film atop iridium heated to $T \leq 700$ K produces a thick carbon film of non-graphitic structure (Fig. 20), which is evidenced by some of its characteristics. First, the shape of the C_{kVV} Auger peak becomes non-graphitic (the spectrum contains one peak at 247 eV, while graphite features two peaks at 247 and 263 eV). Second, adsorption of Cs atoms on such a film does not demonstrate a characteristic splitting of the C_{kVV} Auger peak (a point to be discussed below), which is observed when Cs atoms are adsorbed on a graphite film. Third, the work function increases from 4.45 eV, a figure typical of graphite, to 4.75 eV, an energy identified with chemisorbed carbon. And finally, fourth, the degree of dissociation of CsCl molecules increases from 10^{-4} on graphene to 10^{-1} in the case of a thick carbon film. From this we can infer that adsorption of C atoms on graphene atop iridium heated to 700 K translates into formation of a thick non-graphitic carbon film, which grows on graphene with no intercalation mechanism involved.

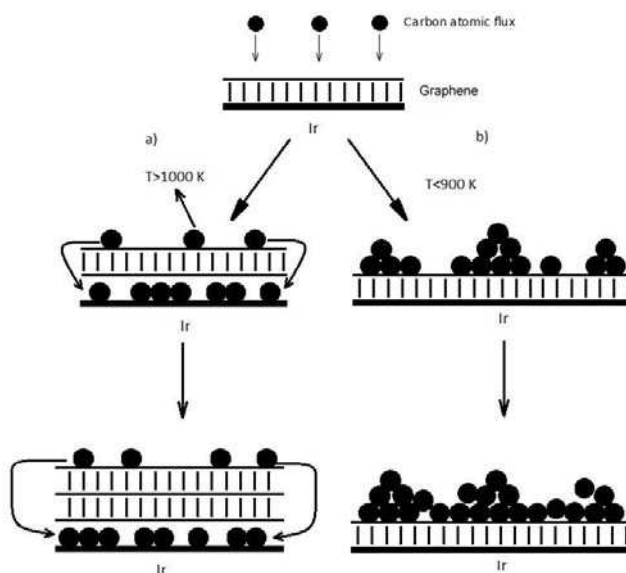


Fig. 20. A scheme of carbon film structure in atomic carbon deposition onto the graphene layer on Ir(111) at various temperatures: (a) - $T > 1000$ K; (b) - $T < 900$ K.

The situation is radically different for the formation of a carbon film when C atoms adsorb on graphene atop iridium heated to higher temperatures, $T \sim 1100$ K (see Fig. 20). Accumulation of carbon in the adlayer likewise was not observed, with all the C atoms striking the surface either intercalating under the graphene islands or desorbing. Intercalation started with formation under the graphene film of graphite islands, and after their coalescence, of a second graphene film above the first one. It was found that after the growth of the second graphene layer has come to completion, the rate of growth of the third graphene layer drops by a few times. This finds a ready explanation in that C atoms have to diffuse from the top of the film to its base, i.e., the iridium surface, where graphene islands of the next layer nucleate; this brings about loss of C atoms because of the increasing

probability of their desorption and of decreasing film growth rate. We note that at $T \leq 700$ K the rate of film growth in thickness is constant for $v_C = \text{const}$. Thus, in adsorption of C atoms on Ir-C at 1100 K carbon accumulates not in the adlayer but rather in intercalated state under the graphene film, where a thick carbon film with graphitic structure grows.

7. Intercalation with silver [25, 26]

Ag was evaporated by sublimation of Ag wires wound on a heated W spiral. Adsorption of silver onto graphene atop iridium did not result in intercalation at any temperature; indeed, at $T < 900$ K, a thick silver film grew, while at $T > 900$ K, silver atoms desorbed. It is possibly because of their tendency to aggregation that Ag atoms form at the edge of a graphite island, a place best suited for starting intercalation, Ag_2 and Ag_3 clusters, which interfere with penetration of silver under the island.

If, however, one intercalates Ir-C preliminarily with Cs atoms to $N \sim 2 \cdot 10^{14} \text{ cm}^{-2}$, and only after this deposits a thick silver film at 300 K and raises then the temperature to 1000 K, then silver will effectively roll off under the graphene in an amount of ~ 1 monolayer, the remaining silver desorbing. It appears reasonable to suggest that silver penetrates under the graphite islands when their edges are raised; it was found that it expels the intercalated cesium.

8. Intercalation with aluminum [27]

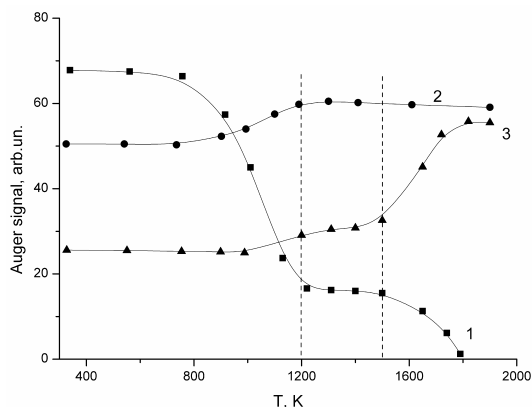
Evaporation of aluminum on graphene atop iridium or rhenium at room temperature brings about growth of three-dimensional aluminum islands on graphite. There is no noticeable intercalation of aluminum under the film, which is evidenced by the Auger signal intensities of carbon and the substrate being attenuated by the growing adsorbate film to the same extent.

The results obtained in annealing of three-dimensional aluminum islands ($N_{Al} \sim \text{cm}^{-2}$) adsorbed on graphene atop iridium are presented in Fig. 21A. We readily see that up to ~ 700 K the system remains practically unchanged. At high temperatures, the Auger signal of aluminum begins to fall off, and that of carbon, to rise, with the substrate (iridium) signal remaining initially constant, to increase slightly afterwards. For $T > 1200$ K, all the three Auger signals reach constant levels remaining unchanged up to 1500 K. At high temperatures, the aluminum signal drops to zero, that of iridium grows almost twofold, and that of carbon, remains unchanged.

To gain understanding of the observed variation of Auger signals, consider Fig. 21B. At $T = 700$ K we see the onset, and at 1200 K, completion of a rearrangement of the adsorption layer, in which three-dimensional aluminum islands adsorbed on top of the graphene layer, dissolve, and the Al atoms released in the process partially evaporate, and partially intercalate under the graphene. For $T > 1200$ K, there is no aluminum on the outer side of the graphene, and the Auger signal of carbon has the same intensity as before the beginning of aluminum evaporation. By contrast, the Auger signal of the substrate became substantially smaller in amplitude as a result of its being screened both by the graphite layer and by the intercalated aluminum; indeed, its intensity is close to one half the initial (before Al evaporation) level (we used the iridium Auger signal with $E = 54$ eV).

With the heating continued ($T > 1500$ K), aluminum escapes from the adlayer, apparently through thermal desorption and, possibly, by partial dissolution in the bulk of the substrate, and its Auger peak drops to zero. By contrast, the Auger peak of iridium grows to its initial level, and that of carbon retains its initial amplitude (Fig. 21A).

A.



B.

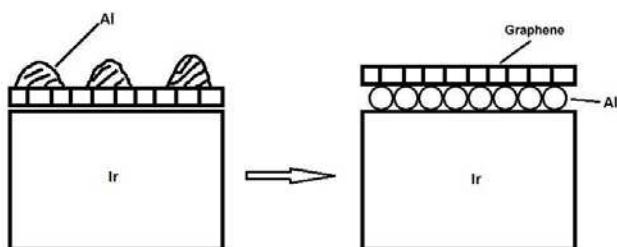


Fig. 21. Al intercalation under a graphene layer on Ir(111). **A.** Auger signals of Al (1), carbon (2), and iridium (3) versus temperature in a stepwise annealing of the Al film deposited onto Ir-C at 300 K. Initial Al surface concentration was $\sim 2 \cdot 10^{15} \text{ cm}^{-2}$. **B.** Schematic structure of the process: at 300 K (left) and at 1200 K (right).

The absolute amount of aluminum intercalated under the film was found to be $N_{\text{Al}} \sim 5 \cdot 10^{14} \text{ cm}^{-2}$ [27].

The net result of direct evaporation of aluminum on graphene at $T > 950 \text{ K}$ is that it ceases to accumulate on top of the graphene layer but intercalates under it instead. This is evidenced by Auger signal of carbon remaining unchanged whereas that of aluminum grows, and the signal of iridium, falls off, albeit insignificantly. This suggests that the aluminum entering the adlayer does not build up on top of the graphite layer and, hence, does not reduce its Auger signal but rather accumulates sandwiched between the graphite film and the metal surface.

An experiment was conducted [27] to measure the efficiency of aluminum intercalation under graphene on (111) iridium, i.e., the fraction of particles penetrating under the film relative to the total number of atoms incident on the surface. Estimates showed the intercalation efficiency to be $\sim 14\%$ at 1000 K, to fall off to 7% at 1100 K. The same figures are obtained when using rhenium as a substrate metal, thus supporting the earlier conclusion of the properties of graphene being practically independent of the nature of the metal it was formed on. The limiting concentration of aluminum accumulating in intercalated state on the surface of rhenium also matches with the composition of the surface aluminide ReAl .

The low efficiency of intercalation should apparently be assigned to desorption of the larger part of the aluminum incident on the surface of graphene. It appeared worthwhile to see whether the aluminum intercalation efficiency would change if graphene covered not all of

the metal surface. For this purpose, we grew successively on a rhenium sample a graphene film of area s covering 40, 70, and 90% of the metal surface, and studied the process of intercalation. The fraction of the substrate surface coated by graphite was assumed to be proportional to the carbon Auger signal intensity from the graphene film.

As follows from these experiments, within experimental error the intercalation efficiency is practically independent of the amount of aluminum that has already penetrated under the film, while remaining dependent on the fraction of the surface coated by the island, to increase at $T = 1100$ K from $W \sim 0.35$ – 0.1 for $s = 90\%$ to $W \sim 1$ for $s < 70\%$. Significantly, the figures obtained exceed by far the efficiency of intercalation of aluminum atoms under a continuous graphene film.

While it would appear reasonable to assume that the quality of the graphene film itself does not depend on whether it is continuous or not, in the second case the number of island boundaries would certainly increase, as would possibly decrease their size. Indeed, the island breakup starts from the edges [3], which is not strange at all, particularly if we remember that the binding energy of a single carbon atom within the layer is ~ 9 eV [28], and at the island edges, substantially lower, ~ 3 eV on rhenium [10] and ~ 4.5 eV on iridium [3]. It may be that the noticeable difference between the efficiencies of intercalation under a monolayer and a submonolayer film suggests that it is the edges of graphene islands that are the defects involved in intercalation of particles under graphene, as was supposed in Ref. [2]. After the islands had coalesced to form a continuous monolayer, the penetration with respect to intercalating particles decreases. And conversely, the increase of the efficiency to a value approaching unity means that the islands have become close in size to the migration path lengths of aluminum atoms they can travel in their lifetimes over graphite surface at a given temperature. Scanning tunneling microscopy suggests that the island size is 3000–8000 Å, and, hence, the migration path lengths of aluminum atoms at 1000–1100 K should be of the same order of magnitude.

The above increase in the intercalation efficiency is very likely of a universal nature, so that it will be characteristic of many types of intercalating particles.

9. Intercalation with iridium [29]

Adsorption of iridium atoms on graphene. Iridium atoms were provided by a second evaporating iridium ribbon, which was freed thoroughly of impurities and heated to ~ 2400 K. The expected flux of Ir atoms subliming from the ribbon was $\sim 10^{15}$ cm $^{-2}$ s $^{-1}$ [30], a level high enough to provide formation of several layers of iridium atoms on graphene surface in a reasonable time.

The main difficulty of the experiment consisted in the need to discriminate by AES the evaporated iridium from the iridium of the substrate. To overcome it, formation of the graphene film was preceded by evaporation on iridium of molybdenum atoms to a concentration of ~ 0.1 of monatomic density (molybdenum is identified adequately by AES). Molybdenum atoms were provided by well cleaned molybdenum ribbons heated to high temperatures. Thus, already after formation of graphene, AES offered a possibility of probing carbon in the form of graphene ($E = 272$ eV), molybdenum ($E = 221$ eV), and iridium ($E = 176$ eV) (Fig. 22a). In these conditions, the intensities of the molybdenum and iridium Auger signals decreased ~ 1.6 times, a figure characteristic of screening by a graphene film [31]. Next, 2–3 layers of iridium were evaporated on graphene at 300 K; this resulted in a decrease of the Auger signal intensities of carbon and molybdenum by about a factor 3 (Fig. 22b).

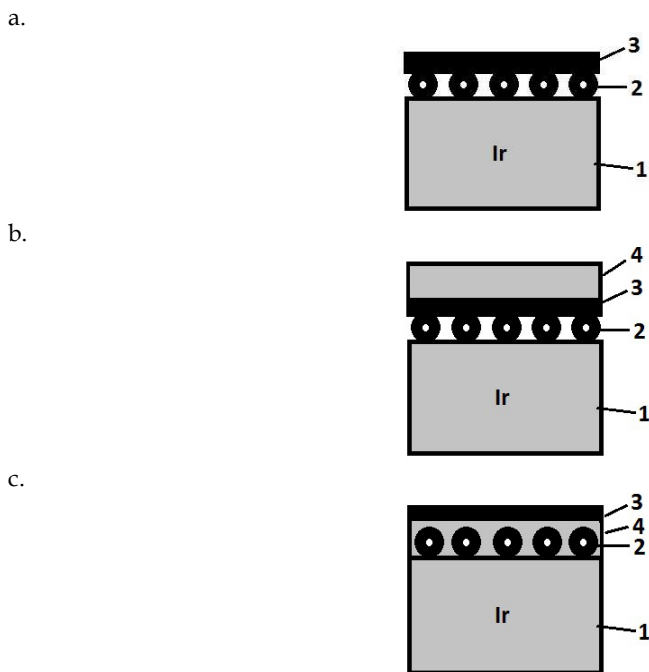


Fig. 22. A model scheme for the adsorption system Ir - graphene with intercalated atomic Mo as an inner standard: **a** - Ir substrate (1) with chemisorbed Mo (2) under graphene (3). Mo surface concentration is ~ 0.1 ML; **b** - the same system with Ir film of ~ 2 ML thickness (4) deposited above the graphene at 300 K; **c** - the result of the system annealing at 1200 K.

Annealing of the Ir(111)-Mo-graphene system. Figure 23 illustrates the results of annealing of an iridium film on graphene obtained by AES. The intensity of the carbon Auger signal at $T = 1100$ K was found to recover to the initial level corresponding to a clean graphene surface. At the same time, the molybdenum Auger signal intensity did not change. This can be understood by examining Fig. 22c. The evaporated iridium has diffused under heating of the sample under the graphene; the graphene surface became free of the adsorbate, with the intensity of the carbon Auger signal growing back to the original level (Fig. 23). At the same time, the iridium film confined under graphene continues to screen the layer of molybdenum, and its Auger signal remains unchanged (Fig. 22c). The decrease of the iridium Auger signal in intensity should apparently be attributed to transition of Ir atoms to the intercalated state and to their screening by the graphene film (Fig. 23).

Direct experiments with evaporation of Ir atoms on graphene performed at moderate temperatures of 1100–1300 K suggest accumulation of iridium under the graphene; indeed, the molybdenum Auger signal intensity decreases, while the surface of graphene remains free of the adsorbate. For $T \geq 1300$ K, desorption of iridium atoms from the heated passive graphene surface begins to play a prominent part, with the result that buildup of Ir atoms in intercalated state decreases strongly.

Experiments with intercalation of graphene with iridium atoms provided supportive evidence for the overall pattern of this process for polyvalent atoms, namely, intensive

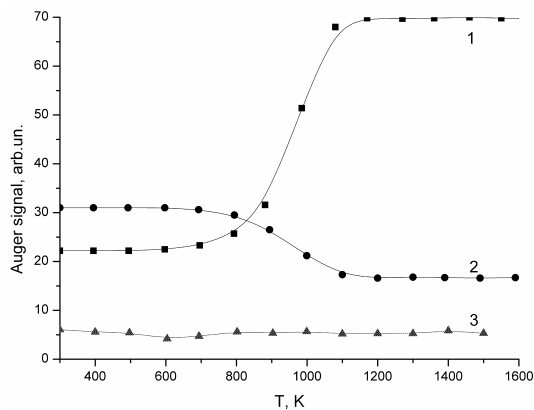


Fig. 23. Carbon (1), Ir (2), and Mo (3) Auger signals versus annealing temperature in a stepwise, within 100 K, heating of the Mo film initially deposited onto graphene at 300 K.

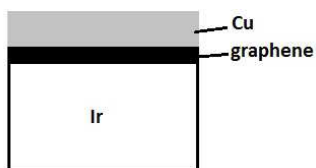
penetration of the adsorbate under the graphene is observed to occur at moderate and high temperatures (1000--1500 K). Recall that atoms with low ionization potentials (primarily the alkali metals) intercalate under graphene at low temperatures, $T \leq 700$ K; also, the lower the temperature, the more efficient is the diffusion of adatoms under the graphene film.

10. Intercalation with copper [32]

Evaporation and annealing of a copper film on iridium. Copper atoms were evaporated on an iridium surface at 300 K until the Auger signal intensity of the substrate dropped to one half its original level, which we estimated as corresponding to a copper concentration of about two monolayers. The main events occurring under stepped annealing of such a film are observed at $T \sim 1100$ K; more specifically, within a narrow temperature interval of the order of 50 K, the Auger signal of copper drops sharply in intensity to melt into the background noise, whereas that of iridium recovers to the original level identified with a clean surface. The most probable mechanism accounting for the surface cleaning is desorption of copper from the iridium surface. While this experiment does not permit us to exclude completely the possibility of copper dissolution in the bulk of the substrate, later experiments with graphene (see below) make this assumption highly unlikely.

Evaporation and annealing of a copper film on graphene atop iridium. Two copper monolayers were evaporated at 300 K on graphene (Fig. 24a), after which the system was annealed in steps at a number of temperatures. The variation of Auger signal intensity from the iridium substrate ($E = 176$ eV), copper ($E = 60$ eV), and carbon ($E = 272$ eV) is displayed in graphical form in Fig. 25. We readily see that at the transition from 1100 to 1200 K the Auger signal of carbon increased sharply to become equal to that from clean graphene surface. There still remains a noticeable Auger signal of copper, though; and since the Auger signal intensity of the substrate is substantially lower than that of the initial, copper-free "graphene on iridium" system, the only reasonable interpretation of the above observations appears to be that copper atoms escaped from the surface under the graphene film to become an intercalant (Fig. 24b). The graphene-involved decrease of the Auger signal of copper ($E = 60$ eV) to about one half its original value suggests that practically all of the

a.



b.



Fig. 24. Schematic structure of the layer transformation for the system Ir(111) - graphene - Cu: (a) - Cu film of ~ 2 ML thickness is deposited upon graphene on Ir(111) ($T=3000\text{K}$); (b) - the same layer after annealing at 1200K .

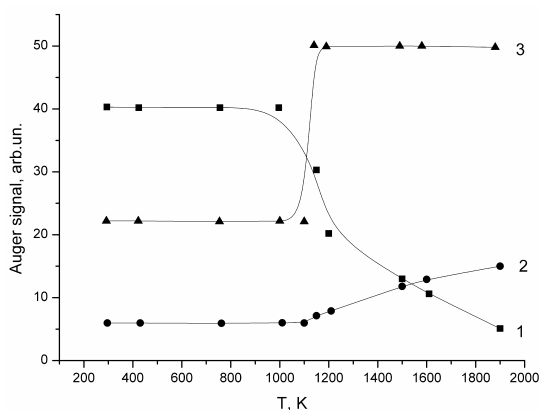


Fig. 25. Cu (1), Ir (2), and carbon (3) Auger signals versus annealing temperature in a stepwise, within 100K , heating of the Cu film initially deposited onto graphene at 300K . Time delay is 30s at each temperature.

copper atoms initially adsorbed on graphene ended with being confined under it [32]. Further annealing brought about one more intriguing observation, namely, the Auger signal of copper is observed now under annealing up to $\sim 1700\text{K}$, i.e., a temperature 500K (sic!) higher than that in the case of clean iridium surface.

This seems to imply that in the first experiment copper atoms mostly desorbed from the clean surface of iridium, whereas in the second experiment the graphene "roof" interferes with this process, with copper atoms left confined to the surface up to high temperatures. Obviously enough, the channel of copper dissolution in the bulk of the metals (if it does exist) remains available in the presence of a graphene film too; moreover, the graphene "roof" which confines Cu atoms at high temperatures ($\geq 1700\text{K}$) enhances the probability for adatoms to dissolve in the bulk of the substrate metal, as this was observed [33] to occur for cesium atoms intercalated in the same iridium-graphene system.

Thus, graphene adsorption on iridium surface acts as a kind of a trap for intercalated copper atoms by increasing substantially the temperature at which the sample is freed completely of the adsorbed atoms.

Graphene acts as a trap for atoms with both high and low ionization potentials, for instance, Cs, K, Na [2, 3, 32]. These two types of systems differ, however, radically from one another. First, atoms of alkali metals intercalate actively under graphene only at low temperatures, $T \leq 700$ K. Second, such atoms can be freed completely from under graphene only if all of the graphene islands break up under heating; the temperatures involved may, however, be quite high indeed—for instance, intercalated cesium escapes from under graphene islands on Re(10-10) at $T \sim 2200$ K (sic!) [2].

In the case of polyvalent atoms and atoms with high ionization potentials, breakup of graphene islands is not required altogether; indeed, the intercalant can escape from under a continuous graphene film through the same defects that were possibly instrumental in its penetration there in the first place (Fig. 26).

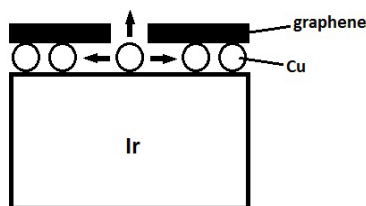


Fig. 26. A model scheme for atomic Cu thermal desorption from the intercalated state.

Now we are turning to the question of why atoms of copper or of other polyvalent high-ionization potential metals diffuse readily under a graphene film on a metal at $T \sim 1100$ – 1200 K, whereas their total removal from the intercalated state requires substantially higher temperatures. It might appear strange that the graphene film behaves in such a, say, anisotropic manner, namely, it is easy to penetrate when atoms transfer from the adsorbed to intercalated state, i.e., from the outer surface inward, but is difficult to cross in the opposite direction,

Let us turn to Fig. 26. As demonstrated by direct studies of migration of Si adatoms on Ir(111), silicon adatoms migrate freely both over a clean iridium surface by wandering from one side of the ribbon to the other (originally clean) in the 1200 K– 1500 K temperature interval, and over iridium with the graphene layer forming [2, 3]; in other words, graphene does not interfere with the migration of adatoms over the metal surface. The same results can be expected with other polyvalent atoms as well (Pt, Cu, Al, etc.); indeed, they migrate easily and uniformly under the graphene film on a metal at temperatures of 1100 – 1200 K.

But then how can an intercalated atom leave an adsorption system? Adatoms in intercalated state get a chance to desorb when two events coincide. First—adatom occurs close to a defect in the graphene film, i.e., on the open surface, as it were, without a graphene roof overhead (Fig. 26). Second—if the adatom receives at exactly this instant a heat pulse from the substrate strong enough to desorb or transfer to the graphene film with subsequent desorption. Otherwise, the adatom will continue its migration further under the graphene film and, even if it is hit by a thermal pulse from the substrate strong enough to break the adsorption bond, will not leave the system, because it will be repelled back from the graphene film. Obviously enough, in this case desorption will become strongly complicated, so that atoms confined under the graphene will be forced to stay in the system up to very

high temperatures. For illustration, Table 3 lists for the Ir(111)-graphene system the temperatures required for the adatoms to escape from a clean metal surface, T_1 , and from the intercalated state, T_2 .

| Element | Cs | K | Al | Cu | Ag |
|-----------|------|------|------|------|------|
| T_1 , K | 900 | 900 | 1500 | 1250 | 1000 |
| T_2 , K | 2000 | 2000 | 1900 | 1900 | 1900 |

Table 3.

Now atoms with low ionization potentials (Cs, K, Na) behave in a radically different way. Diffusion under the graphene film, migration under it and escape from under the graphene are essentially cooperative effects involving electrostatic repulsion of charged adatoms [2, 3]. It can be maintained with confidence that migration of single adatoms of alkali metals under a graphene film is all but suppressed [15].

Thus, the graphene “roof” reduces by many orders of magnitude the probability of desorption of adatoms from the surface compared with that from the open surface of a metal (Table 3).

11. Intercalation with fullerene molecules [34--36]

The density of the flux of C_{60} molecules was estimated from the time taken up by formation of a fullerene monolayer N_M on clean iridium at $T = 300$ K, when the Auger signal intensity of the substrate dropped to one fourth of its initial level, with $\nu_{C60} = N_M/t_M$, where $N_M \approx 2 \cdot 10^{14}$ mol/cm².

If a fullerene monolayer is evaporated at 300 K on graphene atop iridium, the Auger signal intensity of the substrate drops practically down to background level. Heating such a film to $T = 800$ K brings about complete desorption of C_{60} molecules, because one observes recovery of the Auger signals of the graphene film and iridium. Thus, C_{60} molecules do not dissociate on the passive Ir-C surface and do not intercalate with it.

After this, a thick fullerite film ($\sim 3N_M$) was produced on the graphene (Fig. 27a). The intensity of the iridium Auger signal passes into background noise, while the carbon Auger peak took on “fullerene” shape with an energy of 269 eV. The results produced by heating of such a film to 800 K were as follows: only part of the C_{60} molecules desorbed, while a sizable part of C_{60} molecules diffused under the graphene film to become intercalated (Fig. 27b). The disappearance of the iridium Auger signal after the substrate had been heated to 800 K implies that C_{60} molecules had diffused under the graphene in an amount equivalent to not less than one monolayer. The Auger spectrum of carbon was in this case actually a superposition of the Auger spectra of graphene and a fullerene monolayer, with an energy of 271 eV. Experiments on adsorption of C_{60} on clean iridium demonstrated dissociation of C_{60} molecules within the $900 \leq T \leq 1200$ K [37] (Fig. 27C).

In the $1400 \leq T \leq 1600$ K interval, the carbon Auger signal falls off somewhat in intensity, and the substrate Auger signal becomes visible (Figs. 27 c and d). This temperature interval, 1400--1600 K, is associated with active migration of carbon over the surface involving transfer onto the back side of the ribbon (Fig. 27 d), which was supported by direct evidence in studies of migration on clean iridium. For $T > 1600$ K, the carbon film under the graphene undergoes intensive graphitization which changes the C_{kvv} Auger spectrum shape to “graphitic”. At $T = 1600$ --2100 K, the intensity of the Auger signal of carbon can be

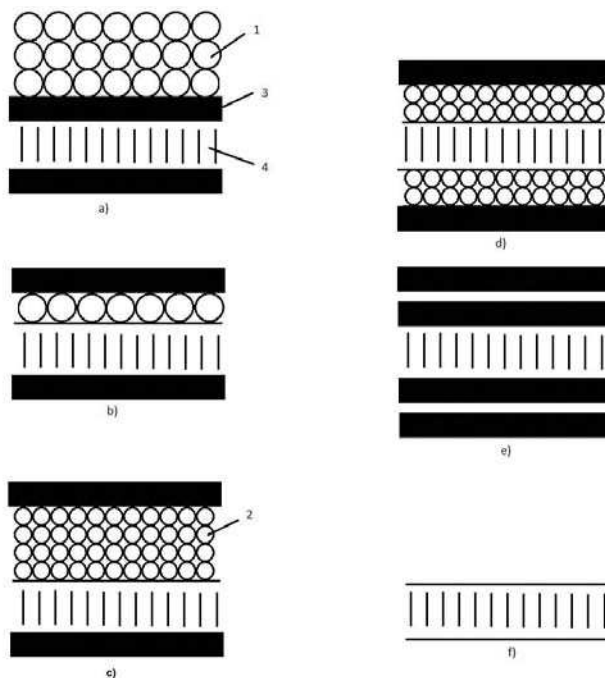


Fig. 27. Schematic representation for intercalation of the graphene layer on Ir(111) by molecular C_{60} . 1 - deposited polylayer film of molecular C_{60} ; 2 - single carbon atom; 3 - graphene layer; 4 - iridium substrate. Temperature, K: (a) - 300; (b) - 800, (c) - 1200; (d) - 1600; (e) - 1900; (f) - 2200.

explained as due to screening by \sim two graphite monolayers (Fig. 27,e). Heating the substrate at temperatures above $T \sim 2200$ K cleaned efficiently the surface of carbon.

Thus, C_{60} molecules adsorbed in the form of a thick fullerite film (unlike a C_{60} monolayer) intercalate under the graphene atop iridium. This might be because the C_{60} molecules at the "bottom" of the fullerite film cannot desorb fast enough at $T = 800$ K and do not break up on the passive graphite surface, but rather transfer by diffusion to the intercalated state.

Graphene on rhenium can be intercalated with fullerene molecules just as this is done with iridium [36].

12. Electronic properties of graphene on metals with adsorbed and intercalated atoms [38--42]

As shown by calculations [43, 44] corroborated by experimental studies of the valence band of single-crystal graphite by photoelectron [45] and Auger electron [46] spectroscopy, the densities of both filled and empty electronic states of two-dimensional graphite drop dramatically close to the Fermi level.

In describing the interaction of particles with the metal surface, we shall follow the scheme suggested by Gurney [47]. As a single atom approaches the surface of a metal, interaction with it broadens the discrete level of the valence electron of the atom into a quasi-level and displaces it from its original position (Fig. 28). In this schematic description, one species of

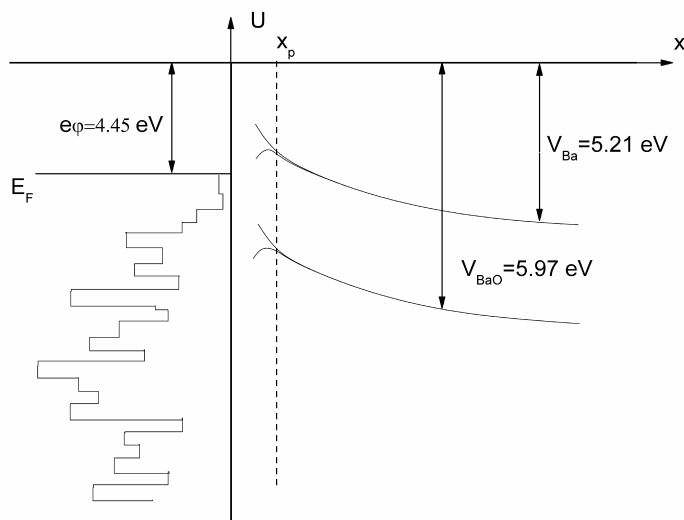


Fig. 28. Schematic transformation of the valence electron level of atomic Ba and molecular BaO in their moving towards the graphene layer on a metal. $e\phi$ is the graphene work function, V - atomic particle ionization potential.

adatoms differs from another in the shape and position of the quasi-level only. The adatom charge is determined both by the position of the center of the quasi-level relative to the Fermi level and its width. For the transfer of valence electrons from Cs and Ba adatoms to the valence band of graphite to be efficient, a sizable part of the quasi-level should be located in both cases above the Fermi level. Adsorption and intercalation with both Cs and Ba adatoms brings about filling of the empty band in the valence band of graphite lying above the Fermi level by depersonalized electrons. It thus appears reasonable to expect that the C_{kvv} Auger transition in two-dimensional graphene involving two electrons from the valence band should be sensitive to its filling. Discussion of the electronic properties of Re-C and Ir-C containing Cs and Ba can be found in Refs. [38--42].

Graphene residing on a metal is made up of atoms of two kinds, adsorbed and intercalated ones, albeit in somewhat different conditions. We start with experiments [28] in which adsorption of Ba atoms on graphene atop iridium heated to 900 K was performed by high-resolution ($\Delta E/E \approx 0.1\%$) AES. It was found that Ba fills only the intercalated state up to high concentrations, $\sim 5 \cdot 10^{14} \text{ cm}^{-2}$, at saturation. As evident from Fig. 29, before the intercalation the C_{kvv} Auger peak has a characteristic graphitic shape with energies 247 and 263 eV in the positive part of the spectrum, but no carbidic peak at the energy 255 eV (spectrum 1). We see that intercalation with Ba does not affect the "graphitic", positive part of the spectrum, while in its negative part, as the Ba concentration increases, first a peak at 276.5 eV (spectra 2 and 5), and after that, a second peak with an energy of 281 eV (spectra 3 and 4) appears on the high-energy side. One may thus conclude that the intercalated Ba is in the charged state, with its valence electron donated to the valence band of graphene to fill the levels adjoining the Fermi level, which is evidenced by the change in the high-energy part of the C_{kvv} Auger peak, because the transition in carbon is the kvv -type, and it involves two electrons of the graphite valence band. A similar pattern was observed in intercalation of HOPG graphite

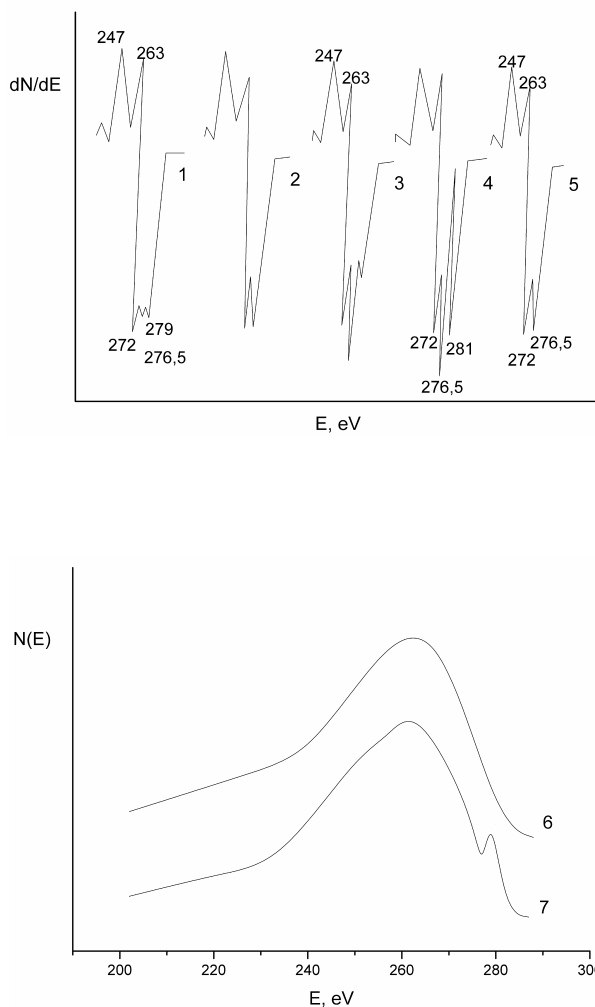


Fig. 29. Carbon KVV differential Auger spectra for sequential stages of Ba adsorption on the graphene layer on Ir(111) at 900 K. Ba concentration under the layer, 10^{14} cm^{-2} : 1 - 0; 2 - 1.5; 3 - 2.5; 4 - 5.0 (saturation). 5 - C_{KVV} Auger spectrum after system annealing at 1600 K ($N_{\text{Ba}} \sim 2 \cdot 10^{14} \text{ cm}^{-2}$). 6; 7 - integral C_{KVV} Auger spectra for pure graphene (6) and for the state 4: Ba adsorption to saturation (7).

with atoms of alkali metals [46, 48]. Heating an Ir-C ribbon to 1600 K forces part of the intercalated Ba to desorb, with the remaining Ba with a concentration of $2 \cdot 10^{14} \text{ cm}^{-2}$ being identifiable with the Auger peak at 276.5 eV (spectrum 5).

Figure 30 [41] presents C_{KVV} Auger spectra obtained in adsorption of Cs on Re-C. This process is paralleled by simultaneous filling of the adsorption (to a concentration N_{α}) and intercalation (to a concentration N_{γ}) states, and at the completion of adsorption, to saturation $N_{\alpha} \sim N_{\gamma} \sim 4$

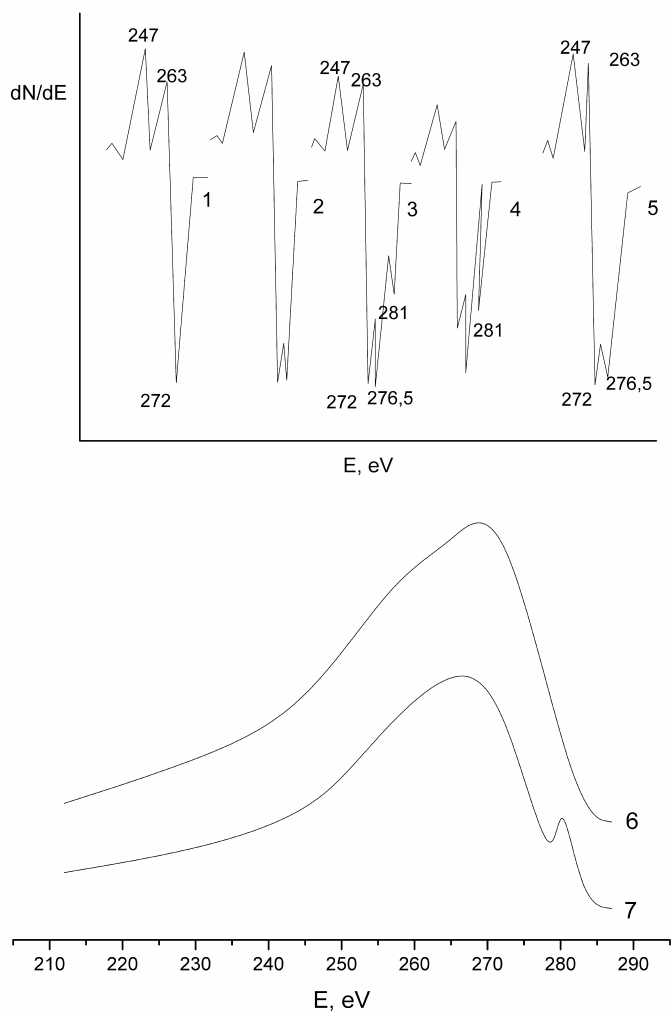


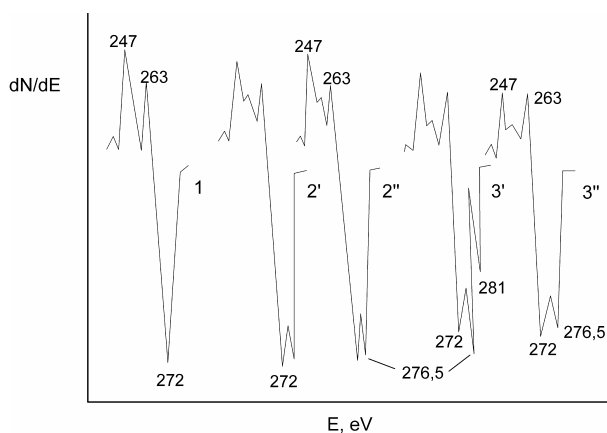
Fig. 30. Carbon KVV differential Auger spectra for sequential stages of Cs adsorption on the graphene layer on Re(10-10) at 300 K. Total Cs concentration over and under the layer, 10^{14} cm^{-2} : 1 - 0; 2 - 1.0; 3 - 2.0; 4 - 7.5 (saturation). 5 - C_{KVV} Auger spectrum after system annealing at 850 K ($N_{Cs} \sim 1 \cdot 10^{14} \text{ cm}^{-2}$). 6; 7 - integral C_{KVV} Auger spectra for pure graphene on Re (6) and for the state 4 - Cs adsorption to saturation (7).

10^{14} cm^{-2} . We readily see that the valence-band electrons of Cs fill the same levels in the graphite valence band as in adsorption of Ba, with peaks at 276.5 eV and 281 eV appearing successively, besides the one at 272 eV, in the negative part of the spectrum.

Interesting relevant information on the behavior of intercalated Cs and Ba with oxygen admitted to the instrument can be found in Ref. [42]. In this experiment, Re-C containing only intercalated Cs, and adsorbed and intercalated Cs was exposed at 300 K to O_2 (with a

dose of 10^{-6} Torr \times 60 s = 60 Langmuirs), and C_{kVV} Auger spectra were recorded (Fig. 31). It turned out that at 300 K the concentration of surface-adsorbed carbon on graphene is as low as to be undetectable by AES (O_2 is only physisorbed on the basal plane of crystalline graphite). Exposure to oxygen did not affect the shape of the C_{kVV} Auger peak of intercalated Cs, wherefrom we can infer that oxygen does not diffuse under the graphite islands on rhenium. Interestingly, the shape of the C_{kVV} peak of adsorbed Cs did change; indeed, the peak at 281 eV disappeared, which implies that as a result of oxidation part of the Cs valence electrons returns from the valence band of graphite into the oxide molecule. Figure 28 illustrates this in the particular example of Ba, in which case oxidation of Ba adatoms on graphene results in formation of a BaO admolecule with its inherent system of electronic levels. It is a safe guess that because of the high ionization potential of the BaO molecule ($V_{BaO} = 6.97$ eV, to be contrasted with $V_{Ba} = 5.21$ eV for the Ba atom) the quasi-level of the valence electron in the BaO admolecule lies below the graphite Fermi level and, thus, will be filled in oxidation by electrons leaving the valence band of graphite.

A.



B.

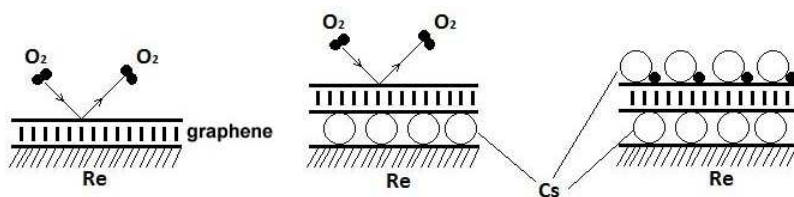


Fig. 31. Cs adsorption on the graphene layer on Re(10-10) at 300 K with subsequent oxidation at $P_{O_2} = 1 \cdot 10^{-5}$ Torr. **A.** Carbon KVV differential Auger spectra. Total Cs concentration over and under the layer, 10^{14} cm^{-2} : 1 - 0; 2' and 2'' - 1.5; 3' and 3'' - 7.0; (saturation). The spectra 2' and 3' are taken before exposure to oxygen; the spectra 2'' and 3'' - after the exposure. **B.** Schematic representation of the process.

An interesting study [42] compared the possibilities of intercalating with cesium the surface of iridium with graphene and a monolayer of chemisorbed carbon with a concentration $N_C \sim 3.9 \cdot 10^{15}$ cm^{-2} produced by adsorption of C atoms on iridium at 300 K. It was found that, in

contrast to graphite, Cs does not intercalate under the monolayer of chemisorbed carbon; indeed, there is no characteristic splitting of the $C_{k_{VV}}$ Auger peak and no high-temperature ($T \geq 2000$ K) γ phase in the TD spectrum.

Another study [41] covered intercalation not only of graphene films on metals with Cs and Ba, but that of thick graphite films on rhenium with cesium at 300 K. Figure 31 presents Auger spectra of graphite on rhenium taken before (spectrum 1) and after (spectrum 2-4a) intercalation with cesium. We readily see that intercalation of both graphene and graphite with cesium atoms initiates similar changes in the shape of the carbon Auger spectrum. As already pointed out, in the case of graphene the strong changes in the shape of carbon Auger peak stem from its unique electronic properties, namely, the layer being two-dimensional, there are many electrons in the valence band, and the levels are widely separated. The same explanation can apparently be assigned to a thick graphite film, because graphene layers are not coupled by electron exchange, and they are bound by van der Waals forces. Incidentally, studying an Auger spectrum of carbon of a similar shape in the case of intercalation into a thick graphite film required a substantially longer exposure time than in the case of one graphene layer. There is nothing strange in it, because as the number of graphite layers increases, the adsorption capacity of the system with respect to cesium which intercalates between all graphite layers increases proportionally. Significantly, heating a graphite film intercalated with cesium to $T \sim 1000$ K removes completely the intercalated cesium (except for the first graphene layer on the metal). We may infer that this heating temperature is high enough to remove cesium both from the surface and from the bulk of graphite, because the edges of graphite "plates" in a thick film are not closed and, thus, do not interfere with diffusion of Cs adatoms with their subsequent desorption.

If a thick, cesium-intercalated graphite film (its Auger spectrum is 4a in Fig. 31) is exposed to oxygen, the Auger peak of cesium decreases by about a factor 5 (from 5a to 5b in Fig. 31), and a high Auger peak of oxygen (6 in Fig. 31) appears in the spectrum. Explanation to this interesting observation can be readily found in that the charged cesium adatoms residing on the outer side of the graphite film become neutralized in the course of oxidation, and, thus, will not interfere with the release of cesium sandwiched inside the graphite film, where cesium adatoms are charged and, hence, repel one another. Thus, a layer of oxide of the alkali metal grows on the surface of the graphite film, whose thickness is large enough to bring about an increase of the Auger peaks of cesium and oxygen and a decrease of that of oxygen. Experiments showed that the thickness of the oxide layer grows with that of the graphite film intercalated with cesium.

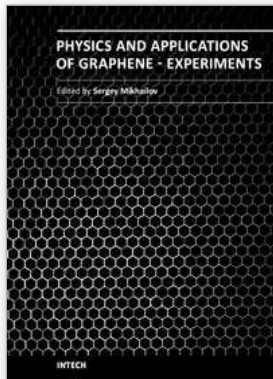
13. References

- E.V. Rut'kov, A.Ya. Tontegode *Pisma Zhur. Tekh. Fiz.*, 7(18), 1122, (1981)
A.Ya. Tontegode, E.V. Rut'kov. *Usp. Fiz. Nauk*, 163(11), 57, (1993)
N.R. Gall, E.V. Rut'kov, A.Ya. Tontegode. *Modern Phys. B.*, 11(16), 1765, (1997)
Graphite Intercalation compounds eds. H.Zabel, S.A.Solin, Springer Ser.Mater.Sci., 1990, v.14; 1992, v.18.
N.A. Kholin, E.V. Rut'kov, A.Ya. Tontegode. *Surf. Sci.*, 139, 155, (1984)
J.E.Fischer, R. Thomson, *Phys.Today*, 1978, v.31, N.7, p.363.
N.R. Gall, E.V. Rut'kov, S.N. Mikhailov, A.Ya. Tontegode *Fiz. Tverd. Tela*. 27(8), 2351, (1985)

- N.R. Gall, S.N. Mikhailov, E.V. Rut'kov, A.Ya. Tontegode *Zhur. Tekn. Fiz.*, 56, 732, (1986)
- N.R. Gall, S.N. Mikhailov, E.V. Rut'kov, A.Ya. Tontegode *Surf. Sci.*, 191, 185, (1987)
- N.R. Gall, S.N. Mikhailov, E.V. Rut'kov, A.Ya. Tontegode *Fiz. Tverd. Tela*, 28, 2521, (1986)
- N.R. Gall, S.N. Mikhailov, E.V. Rut'kov, A.Ya. Tontegode *Synthetic Metals*, 34, 497, (1989)
- E.V. Rut'kov, N.R. Gall, *Fiz. Tverd. Tela* 51(8), 1639 (2009)
- E.V. Rut'kov, N.R. Gall. *Pisma Zhur. Eksp. Tekn. Fiz.* 88(4), 308, (2008)
- M.S. Dresselhaus, G. Dresselhaus. *Advan. Phys.* 30, 139, (1981)
- M.V. Knat'ko, V.I. Paleev, N.D. Potehina *Zhur. Tekn. Fiz.* 59, 154, (1989)
- A. Ya. Tontegode *Pisma Zhur. Tekn. Fiz.*, 15, 57, (1989)
- E.V. Rut'kov, A.Ya. Tontegode *Zhur. Tekn. Fiz.*, 45(9), 1884, (1975)
- E.V. Rut'kov, A.Ya. Tontegode *Fiz. Tverd. Tela*, 32(10), 2960, (1990)
- E.V. Rut'kov, A.Ya. Tontegode *Materials Science Forum*, (91-93), 709, (1992)
- E.Y. Zandberg, E.V. Rut'kov, A.Ya. Tontegode *Pisma Zhur. Tekn. Fiz.*, 1(16), 741, (1975)
- E.Y. Zandberg, E.V. Rut'kov, A.Ya. Tontegode, N.D. Potehina *Fiz. Tverd. Tela*, 19(2), 1665, (1997)
- N.R. Gall, E.V. Rut'kov, A.Ya. Tontegode, *Pisma Zhur. Tekn. Fiz.* 14(6), 527, (1988)
- N.R. Gall, E.V. Rut'kov, A.Ya. Tontegode *Povrkhnost*, 10, 47, (1989)
- N.R. Gall, E.V. Rut'kov, A.Ya. Tontegode *J. Chemical Vapor Deposition*, July, 6(1), 72, (1997)
- N.R. Gall, E.V. Rut'kov, A.Ya. Tontegode *Pisma Zhur. Eksp. Tekn. Fiz.*, 75(1), 28, (2002)
- N.R. Gall, E.V. Rut'kov, A.Ya. Tontegode *Phys Solid State*, 46(2), 371, (2004)
- N.R. Gall, E.V. Rut'kov, A.Ya. Tontegode *Semiconductors*. 36(3), 276, (2002)
- A.R.Ubbelohde, F.A.Lewis, "Graphite and its Crystal compounds", Oxford, Clarendon Press, 1960.
- E.V. Rut'kov, N.R. Gall *Pisma Zhur. Tekn. Fiz.* 35 (16), 1 (2009)
- N.A.Nesmeianov "Vapor pressure of chemical elements", Academia Nauk Publ., Moscow, 1961. (in Russian)
- V.N. Ageev, E.V. Rut'kov, A.Ya. Tontegode, N.A. Kholin *Fiz. Tverd. Tela*, 23(8), 2248, (1981)
- E.V. Rut'kov, N.R. Gall *Fiz. Tekn. Poluprovodnikov*, 43(10), 57 (2009)
- A.Ya. Tontegode, F.K. Yusifov *Fiz. Tverd. Tela*, 35, 987, (1993)
- E.V. Rut'kov, A.Ya. Tontegode, M.M. Usufov, Yu.S. Grushko *Mol. Mat.*, 4, 217, (1994)
- E.V. Rut'kov, A.Ya. Tontegode, M.M. Usufov *Phys. Rev. betters* 74(5), 758, (1995)
- N.R. Gall, E.V. Rut'kov, A.Ya. Tontegode, M.M. Usufov, *Mol. Mat.*, 7, 187, (1996)
- E.V. Rut'kov, A.Ya. Tontegode, Yu.S. Grushko *Pisma Zhur. Eksp. Tekn. Fiz.* 57(11), 712, (1993)
- N.R.Gall, S.N. Mikhailov, E.V. Rut'kov, A.Ya. Tontegode *Poverkhnost*, 12, 14, (1986)
- N.R.Gall, S.N. Mikhailov, E.V. Rut'kov, A.Ya. Tontegode *Fiz. Tverd. Tela*, 28(8), 2521, (1986)
- N.R.Gall, S.N. Mikhailov, E.V. Rut'kov, A.Ya. Tontegode *Poverkhnost*, 4, 22, (1987)
- N.R.Gall, S.N. Mikhailov, E.V. Rut'kov, A.Ya. Tontegode *Synthetic Metals*, 34(1-3), 447, (1989)
- N.R.Gall, S.N. Mikhailov, E.V. Rut'kov, A.Ya. Tontegode *Surf. Sci.*, 226, 381, (1990)
- R.F. Willis, B.E. Fitton, G.S. Painter *Phys. Rev.*, 9, 1926, (1974)
- G.S. Painter, D.E. Ellis *Phys. Rev.* 1, 4797, (1970)
- P. Murchand, G. Fretigny, M. Lagies and al. *Phys. Rev.*, 30, 4788, (1984)
- P. Oelhafen, P. Pfluger, H.I. Gr ntherodt *Solid State Commun.*, 32, 885, (1975)

R. Gurney *Phys. Rev.*, 47, 479, (1935)

P. Pfluger, P. Oelhafen, N.H. Künzi, R. Ieker, E. Hauser, K.P. Ackermann, M. Müller, H.I. Cüntheoront *Physica B+C*, 99, 395, (1980)



Physics and Applications of Graphene - Experiments

Edited by Dr. Sergey Mikhailov

ISBN 978-953-307-217-3

Hard cover, 540 pages

Publisher InTech

Published online 19, April, 2011

Published in print edition April, 2011

The Stone Age, the Bronze Age, the Iron Age... Every global epoch in the history of the mankind is characterized by materials used in it. In 2004 a new era in material science was opened: the era of graphene or, more generally, of two-dimensional materials. Graphene is the strongest and the most stretchable known material, it has the record thermal conductivity and the very high mobility of charge carriers. It demonstrates many interesting fundamental physical effects and promises a lot of applications, among which are conductive ink, terahertz transistors, ultrafast photodetectors and bendable touch screens. In 2010 Andre Geim and Konstantin Novoselov were awarded the Nobel Prize in Physics "for groundbreaking experiments regarding the two-dimensional material graphene". The two volumes Physics and Applications of Graphene - Experiments and Physics and Applications of Graphene - Theory contain a collection of research articles reporting on different aspects of experimental and theoretical studies of this new material.

How to reference

In order to correctly reference this scholarly work, feel free to copy and paste the following:

E.V.Rut'kov and N.R.Gall (2011). Intercalation of Graphene Films on Metals with Atoms and Molecules, Physics and Applications of Graphene - Experiments, Dr. Sergey Mikhailov (Ed.), ISBN: 978-953-307-217-3, InTech, Available from: <http://www.intechopen.com/books/physics-and-applications-of-graphene-experiments/intercalation-of-graphene-films-on-metals-with-atoms-and-molecules>

INTECH
open science | open minds

InTech Europe

University Campus STeP Ri
Slavka Krautzeka 83/A
51000 Rijeka, Croatia
Phone: +385 (51) 770 447
Fax: +385 (51) 686 166
www.intechopen.com

InTech China

Unit 405, Office Block, Hotel Equatorial Shanghai
No.65, Yan An Road (West), Shanghai, 200040, China
中国上海市延安西路65号上海国际贵都大饭店办公楼405单元
Phone: +86-21-62489820
Fax: +86-21-62489821

© 2011 The Author(s). Licensee IntechOpen. This chapter is distributed under the terms of the [Creative Commons Attribution-NonCommercial-ShareAlike-3.0 License](#), which permits use, distribution and reproduction for non-commercial purposes, provided the original is properly cited and derivative works building on this content are distributed under the same license.